

TWO PHASE FLOW AND HEAT TRANSFER
IN POROUS BEDS UNDER VARIABLE
BODY FORCES

N70 32924

CR- 102788

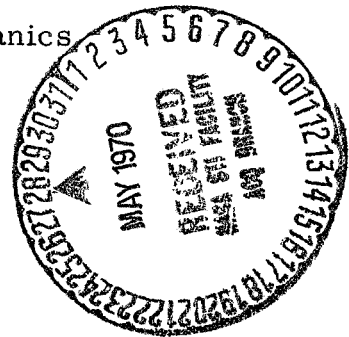
Final Report

Part V

By James V. French, Jr. and Harold R. Henry

Project Director:

Harold R. Henry, Ph.D.
Professor of Engineering Mechanics
University of Alabama



Submitted to

George C. Marshall Space Flight Center
National Aeronautics and Space Administration
Huntsville, Alabama

Contract No. NAS8-21143
University of Alabama No. 22-6560

December 1969
Bureau of Engineering Research
University of Alabama

CASE FILE
COPY

Report No. 113-30
Part V

TWO PHASE FLOW AND HEAT TRANSFER
IN POROUS BEDS UNDER VARIABLE
BODY FORCES

Final Report

Part V

By James V. French, Jr. and Harold R. Henry

Project Director:

Harold R. Henry, Ph.D.
Professor of Engineering Mechanics
University of Alabama

Submitted to

George C. Marshall Space Flight Center
National Aeronautics and Space Administration
Huntsville, Alabama

Contract No. NAS8-21143
University of Alabama No. 22-6560

December 1969
Bureau of Engineering Research
University of Alabama

TABLE OF CONTENTS

	Page
LIST OF FIGURES	iii
LIST OF SYMBOLS	vi
PREFACE	viii
I. INTRODUCTION	1
Introduction to Two-Phase Flow	1
Qualitative Description of Gas-Liquid Flow	2
Problems in Metering Two-Phase Flow	3
Purpose and Scope of This Study	4
II. THEORETICAL BASIS	6
Darcy Two-Phase Flow	6
Functional Relations for Gas-Liquid Two-Phase Flow Through Porous Cartridges	9
Theoretical Flowmeter Calibrations	13
III. EXPERIMENTAL APPARATUS	17
Test Section	17

Porous Cartridges	19
Supporting Test Equipment	20
IV. EXPERIMENTAL PROCEDURE	24
V. EXPERIMENTAL RESULTS	27
General Results	27
Presentation of Data	28
Effects of Flow Patterns	33
Sources of Error	35
VI. CONCLUSIONS AND RECOMMENDATION	38
FIGURES	41
BIBLIOGRAPHY	71
ADDITIONAL DATA	73

LIST OF FIGURES

Table	Page
1. Gradation of Glass Beads	41
Figure	
1. Typical Relative Permeability Curves	42
2. Porous Cartridge Arrangement in Two-Phase Flow Channel	43
3a. Hypothetical Experimental Data	44
3b. Hypothetical Calibration Curves	44
4. Assembly Drawing of Test Section	45
5. Porous Cartridges - Configuration I	46
6. Porous Cartridges - Configuration II	47
7. Porous Cartridges - Configuration III	48
8. Porous Cartridges - Configuration IV	49
9. Schematic Diagram of Experimental Apparatus for Two-Phase Flow-Meter Calibration	50
10. Test Bench	51
11. Experimental Data - Configuration II - 0°, Cartridge No. 1	53

List of Figures (Continued)	Page
12. Experimental Data - Configuration II - 0°, Cartridge No. 2	54
13. Calibration Data - Configuration II - 0°	55
14. Experimental Data - Configuration II - 180°, Cartridge No. 1	56
15. Experimental Data - Configuration II - 180°, Cartridge No. 2	57
16. Calibration Data - Configuration II - 180°	58
17. Experimental Data - Configuration IV - 0°, Cartridge No. 1	59
18. Experimental Data - Configuration IV - 0°, Cartridge No. 2	60
19. Calibration Data - Configuration IV - 0°	61
20. Experimental Data - Configuration IV - 180°, Cartridge No. 1	62
21. Experimental Data - Configuration IV - 180°, Cartridge No. 2	63
22. Calibration Data - Configuration IV - 180°	64
23. Idealized Calibration Data	65
24. Experimental Data - Configuration IV, Cartridge No. 1	66
25. Experimental Data - Configuration IV, Cartridge No. 2	67
26. Photographs of the Test Section in Upward Two-Phase Flow	68

List of Figures (Continued)	Page
27. Photographs of Upward Two-Phase Flow	69
28. Photographs of the Porous Cartridges in Downward Two-Phase Flow	70
29. Meter with Porous Cartridges of Different Diameters	75
30. Experimental Data for Meter of Figure 29	76
31. Experimental Data for Meter of Figure 29	77
32. Calibration Chart for Meter of Figure 29	78

LIST OF SYMBOLS

A	Area	in ²
d	Pore Size	in
g	Acceleration due to Gravity	ft/sec ²
H	Pressure Gradient	psi/in
K	Permeability	ft ²
K _g	Permeability of Porous Medium to Gaseous Phase	ft ²
K _L	Permeability of Porous Medium to Liquid Phase	ft ²
k	Relative Permeability	
k _g	Relative Permeability of Porous Medium to Gaseous Phase	
k _L	Relative Permeability of Porous Medium to Liquid Phase	
L	Length	in
ṁ _g	Mass Flowrate of Gaseous Phase	slugs/min
ṁ _L	Mass Flowrate of Liquid Phase	slugs/min
p	Pressure	lb/in ²
q	Volumetric Flowrate	ft ³ / min
q _g	Volumetric Flowrate of Gaseous Phase	ft ³ / min

q_L	Volumetric Flowrate of Liquid Phase	gal/min
R	Gas Constant	ft-lb/lb- $^{\circ}$ R
S	Saturation Ratio	
S_g	Gaseous Saturation Ratio	
S_L	Liquid Saturation Ratio	
T	Temperature	$^{\circ}$ R
v	Volumetric Flowrate per Unit Area	ft/min
v_g	Volumetric Flowrate per Unit Area of Gaseous Phase	ft/min
v_L	Volumetric Flowrate per Unit area of Liquid Phase	ft/min
y	Elevation above Datum	ft
θ	Porosity	
μ	Viscosity	lb-sec/ft ²
ρ	Density	slugs/ft ³
σ	Surface Tension	lb/ft
∇	Vector Operator Del	1/in

PREFACE

This is Part V of a seven part Final Report on work under Contract No. NAS8-2143 between the George C. Marshall Space Flight Center and the University of Alabama. This report includes the results of experiments to determine the feasibility of using two dissimilar porous cartridges in series with appropriate instrumentation to constitute a two-phase mass flow meter. It also includes a discussion of the functional relationships among the variables involved.

The correlation of experimental data indicates that the meter can be calibrated for a particular gas and liquid by a series of runs in which the flow rates of the gas and liquid are separately metered, the pressure drop across each cartridge is measured and the temperature and absolute pressure in the space between cartridges is recorded.

The calibration chart is constructed when the pressure drop across one cartridge is plotted against the pressure drop across the other cartridge for constant values of liquid flow rate as is shown, for instance, in Figures 19, 22 and 32. Figure 32 is the most complete calibration chart because it has curves for constant gas mass flow rate superimposed so that a separate chart for this quantity is not required.

This meter, with no moving parts and very little pressure drop, provides a method of utmost simplicity for the determination of the mass flow rates of the individual components when a two-phase mixture is flowing. The importance of this in space technology is evident when one takes note of the many instances of two-phase flow in flight situations where it is extremely difficult to separate the gas from the liquid.

I. INTRODUCTION

Introduction to Two-Phase Flow

A two-phase system may consist of any one of four basic types, namely: a gas and a liquid, a gas and solid particles, a liquid and solid particles, and two immiscible liquids. In the case of a gas-liquid system both phases may be continuous and separated by an interface or one phase may be continuous while the other has the form of bubbles or droplets. Although the principal gas may be foreign to the liquid the vapor phase of the liquid will be present in an amount depending upon the temperature. Suspensions of small solid particles in a gas or liquid comprise the second and third categories respectively. The case of two immiscible liquids may be subdivided into two different types, namely: one liquid existing as droplets in the other or both phases may be continuous and separated by an interface [14]¹.

There is much current interest in the areas of gas-liquid and liquid-liquid systems due to applications in the areas of heat transfer, chemical processes, ground water technology, and oil and gas field

¹Numbers in square brackets refer to references at the end of the thesis.

management. The study of gas-liquid systems may be approached either from the viewpoint of bubble dynamics where the attention is focused upon the action of individual particles or by a bulk treatment of the two-phase mixture as a whole. Examples of the latter type of study for pipe flow are the papers of Lockhart and Martinelli [9], Moody [11], and Nicklin [12]. Representative investigations for gas-liquid flow in packed porous beds are the papers by Gorring and Katz [3], Weekman and Myers [16], and the unpublished notes of Henry, Chow, and Bates [8]. A generalized theoretical approach to multiphase flow in porous media was made by Wyllie and Gardner [17], [18]. The flow of two miscible liquids in porous media has been studied by assuming a sharp non-capillary interface by Henry [4], [6]. Papers in the related field of a single liquid with density gradients in a porous medium include those of Henry [5], [7] and Miller [10].

Qualitative Description of Gas-Liquid Flow

Since the experimental investigation was concerned with a gas-liquid system, it is appropriate to discuss the qualitative aspects of gas-liquid flow systems in pipe flow. A qualitative description of gas-liquid flow may be based upon the flow pattern within a pipe or tube. Here, flow pattern means the physical arrangement of the gas

and liquid phases within a section of pipe. Although many flow patterns may be identified, for the sake of simplicity they may be grouped into the following three classifications: bubble flow, slug flow, and annular flow. For given gas and liquid properties the flow pattern will be determined by the volumetric flowrates of each phase and the direction of the buoyancy force relative to the flow direction. Usually, bubble flow occurs at low ratios of gas flowrate to total flowrate with slug flow at intermediate ratios, and annular flow occurring at the higher ratios of gas flowrate to total flowrate. In bubble flow the liquid phase is continuous and the gas takes the form of individual bubbles. Slug flow is said to exist when relatively large volumes of liquid occur followed by correspondingly large volumes of gas. The flow is basically unstable due to rapid changes of density. Flow in a closed channel is termed annular flow when the liquid phase is continuous in an annulus along the wall and the gaseous phase is continuous in the central region [15].

Problems in Metering Two-Phase Flow

Conventional methods of flowrate measurement in general are not satisfactory for two-phase flow due to the discontinuous density of the two-phase mixture. Several types of mass flowmeters used for cryogenic fluids also hold some promise for general two-phase

use. In this category are those meters which combine a measurement of the fluid velocity in a pipe with some other measurement of density such as electrical capacitance or a weighing method. Methods which measure the velocity of a liquid in a pipe such as tracer injection and the electromagnetic flowmeter, which measures an induced emf due to the velocity of a conducting liquid in a magnetic field, are limited by the fact that the liquid and gas do not in general have the same velocity. Perhaps the best method at the present time for mass flowrate measurements in two-phase flow is the mass reaction type of meter. In this type, a change of momentum is forced upon the flowing stream either by an impeller or by rotation of a loop of pipe through which the two-phase mixture flows. A measure of the torque required to cause a given change in momentum gives an indication of the mass flowrate. A disadvantage of this method lies in the difficulty of obtaining an accurate measurement of the torque and in the relatively complicated mechanical design of the system [1].

Purpose and Scope of this Study

The purpose of this investigation is to determine if it is feasible to develop a flowmeter for use in gas-liquid two-phase flow which uses as its primary sensing elements, two porous cartridges through which the flow passes in series. This concept is based upon the

experimental fact that porous media exhibit selective relative permeabilities to each fluid in Darcy flow of two immiscible fluids. A library search and review of current books in the fields of flow through porous media and multiphase flow have revealed no reference to this method of metering two-phase flow.

The fluids selected for this study were water and air at approximately room temperature and gage pressures up to 35 psig. The range of flowrates was limited to those which required a pressure drop of 35 psi or less through the test section. Also the flowrate of the gas was limited by the beginning of large system instabilities which could not be accurately recorded with the existing test equipment. No effort was made to study the liquids at or near their boiling points such that the principal constituent of the gaseous phase would be the liquid vapor.

II. THEORETICAL BASIS

Darcy Two-Phase Flow

For a certain range of flow of a single incompressible fluid through a homogeneous porous medium, Darcy's law is well established. In general it is agreed that Darcy's law is valid for flows having a Reynolds number less than unity based upon bulk velocity and average pore size of the porous medium [2], [13]. In vector form Darcy's equation may be written as,

$$\vec{v} = - \frac{K}{\mu} \nabla(p + \rho gy) \quad (1)$$

where \vec{v} is the vector volumetric flowrate per unit area, K is the permeability of the porous medium and is independent of the particular fluid being used, μ is the viscosity of the fluid, p is pressure, ρ is the density of the fluid, g is the acceleration due to gravity, y is the elevation above datum, measured positive upward, and ∇ is the vector operator del.

For simultaneous flow of immiscible fluids through porous media, Darcy's Law is not valid in the form given above. However,

if the Reynolds number is less than one for each phase, an equation of the same form as equation (1) can be written for each phase if the permeability is replaced by an experimentally obtained coefficient which will, in general, be a function of the flow parameters. This experimental coefficient is commonly called the effective permeability for a given phase. These equations for each phase are of the form of Darcy's equation and may be called extensions of Darcy's equation for flow of two immiscible fluids. The extended Darcy's law for each fluid gives the flowrate per unit area in terms of the effective permeability, viscosity, and the pressure gradient. Although most of the experimental data has been obtained on liquid-liquid systems, under certain conditions this concept may be applied to gas-liquid flow. If the average pressure is large enough so that slip flow does not occur and the compressibility of the gas is considered, effective permeabilities of each phase may be defined as in the liquid-liquid case.

For convenience, relative permeabilities are defined as follows: if K_L and K_g are the effective permeabilities of a porous medium to the liquid and gas phases respectively of a two-phase flow system, then the respective relative permeabilities are

$$k_L = \frac{K_L}{K} , \quad k_g = \frac{K_g}{K} \quad (2), (3)$$

where K is the permeability of the porous medium to a single fluid. For laminar flow the relative permeabilities are functions of the fraction of the total pore volume occupied by each fluid. This quantity may be called the saturation ratio, S . Figure 1 is a typical plot of relative permeabilities versus saturation ratio [2], [15]. If it is assumed that all of the pores are filled by one phase or the other,

$$S_L + S_g = 1 \quad (4)$$

Using the relative permeability concept, the vector flowrates per unit area of each phase in gas-liquid flow may be written as,

$$\vec{v}_L = - \frac{k_L K}{\mu_L} \nabla(p + \rho gy) \quad (5)$$

$$\vec{v}_g = - \frac{k_g K}{\mu_g} \nabla(p + \rho gy) \quad (6)$$

All of the above relationships are based upon the requirement that the Reynolds number be less than one. If the flow is out of this range and there is no longer a linear relationship between velocity and pressure gradient, Darcy's law does not apply. In analogy to pipe flow, it has been suggested that the pressure gradient

be represented by a linear combination of a first order and a second order term in velocity, with the coefficients being functions of the flow parameters [13]. This is the simplest type of relationship which would appear to agree with experimental data, but several other more complex forms are given in the literature [13], [17], [18]. An alternate method to that of developing a definite mathematical model for flow outside the Darcy range is to consider general functional relationships among the parameters governing the flow. Useful information can be obtained in this manner even though the exact mathematical forms are not known. In the following section this concept is used to formulate a theoretical basis for metering of gas-liquid flow using two porous cartridges.

Functional Relations for Gas-Liquid Two-Phase Flow Through Porous Cartridges

Consider the case of one-dimensional flow of a gas-liquid mixture through a porous cartridge placed in a pipe. The characteristics of the cartridge which should be considered include: the porosity, θ ; the average pore size, d ; the area perpendicular to the flow direction, A ; and the length parallel to the flow direction, L . The properties of each phase that should be considered are: viscosity, μ ; density, ρ ; and the surface tension of the interface between the two phases, σ . Let the pressure gradient across the cartridge be

denoted by H and let q_L be the volumetric flowrate of the liquid phase and q_g be the volumetric flowrate of the gaseous phase, measured at the average pressure in the cartridge.

Observing the form of equations (5) and (6) and recalling the dependence of relative permeability upon saturation ratio as shown by Figure 1, it is reasonable to assume that the flowrate of one phase of a two-phase flow through a porous cartridge will be a function of the pressure gradient, the properties of the porous cartridge, the properties of the fluids, and of the saturation ratio. If the velocities of the two phases were equal within the porous material, the gas saturation ratio, S_g , would be given by the ratio of the volumetric gas flowrate to the total two-phase volumetric flowrate, but in general these velocities will not be equal and

$$S_g \neq \frac{q_g}{q_g + q_L} . \quad (7)$$

However, laboratory investigations indicate that a definite functional relationship does exist between saturation ratio and the flowrates of each phase [8]. The graphical presentation of this relationship as presented in reference [8] may be written functionally as,

$$S_g = F \left(\frac{q_g}{q_g + q_L}, q_L \right) . \quad (8)$$

For general two-phase flow through a porous cartridge, it may be assumed that functional relationships for the flowrates of each phase may be written in the following form:

$$q_L = F_L \left(H, \frac{q_g}{q_g + q_L}, \mu_L, \mu_g, \rho_L, \rho_g, \theta, A, L, d, \sigma \right) \quad (9)$$

$$q_g = F_g \left(H, \frac{q_g}{q_g + q_L}, q_L, \mu_L, \mu_g, \rho_L, \rho_g, \theta, A, L, d, \sigma \right). \quad (10)$$

Using the common assumption that the pressure is constant in a cross section in pipe flow [11], then H is common to both (9) and (10). This condition results in equations (9) and (10) being no longer independent as is shown in Chapter V. Thus the functional relationship among the variables can be written as:

$$H = G \left(q_L, \frac{q_g}{q_g + q_L}, \mu_L, \mu_g, \rho_L, \rho_g, \theta, A, L, d, \sigma \right), \quad (11)$$

If dimensional analysis is applied to the variables in expression (11), the following nondimensional groups may be formed:

$$\frac{H d^4}{\mu_L q_L}, \frac{q_L \rho_L d}{A \mu_L}, \frac{q_g}{q_L + q_g}, \frac{H d^2}{\sigma}, \frac{\mu_L}{\mu_g},$$

$$\frac{\rho_L}{\rho_g}, \theta, \frac{A}{d^2}, \frac{L}{d}.$$

Equation (11) then may be written as:

$$\frac{H d^4}{\mu_L q_L} = G' \left(\frac{q_L \rho_L d}{A \mu_L}, \frac{q_g}{q_L + q_g}, \frac{H d^2}{\sigma}, \frac{\mu_L}{\mu_g}, \right.$$

$$\left. \frac{\rho_L}{\rho_g}, \theta, \frac{A}{d^2}, \frac{L}{d} \right). \quad (12)$$

If the properties of the porous cartridges are known and the fluid properties are specified by measurement of pressure and temperature, expression (12) relates the three variables H , q_g , and q_L . Therefore, if any two of these quantities are known, the third may be determined from an expression of the form of (12). Equation (12) is a mathematical statement of a basic hypothesis of this study: given a porous medium with known properties and a two-phase system flowing through it, there exists a functional relationship between the pressure gradient and the flowrates of each phase so that the specification of any two of these quantities uniquely determines the third. In the following section it is shown how this concept may be used to

form a two-phase flowmeter using two porous cartridges.

Theoretical Flowmeter Calibration

Consider two porous cartridges placed in a pipe so that all of a two-phase mixture flows through each in turn as shown schematically in Figure 2. The porous medium composing each may be different and the physical dimensions may be different for each cartridge, so that the flow characteristics through each one are also different.

Although the flows are dissimilar, assume that each obeys a relationship like equation (12) so that,

$$\left(\frac{H d^4}{\mu_L q_L} \right)_1 = G_1 \left[\left(\frac{q_L \rho_L d}{A \mu_L} \right)_1 , \left(\frac{q_g}{q_L + q_g} \right)_1 , \left(\frac{H d^2}{\sigma} \right)_1 , \right. \\ \left. \left(\frac{\mu_L}{\mu_g} \right)_1 , \left(\frac{\rho_L}{\rho_g} \right)_1 , \theta_1 , \left(\frac{A}{d^2} \right)_1 , \left(\frac{L}{d} \right)_1 \right] , \quad (13)$$

$$\left(\frac{H d^4}{\mu_L q_L} \right)_2 = G_2 \left[\left(\frac{q_L \rho_L d}{A \mu_L} \right)_2 , \left(\frac{q_g}{q_L + q_g} \right)_2 , \left(\frac{H d^2}{\sigma} \right)_2 , \right. \\ \left. \left(\frac{\mu_L}{\mu_g} \right)_2 , \left(\frac{\rho_L}{\rho_g} \right)_2 , \theta_2 , \left(\frac{A}{d^2} \right)_2 , \left(\frac{L}{d} \right)_2 \right] . \quad (14)$$

If (13) and (14) are independent equations, for a given set of two porous cartridges and a two-phase system with specified properties, a set of four variables; q_g , q_L , H_1 , and H_2 , related by two

independent equations is formed. The condition that (13) and (14) be independent could be obtained by requiring some of the parameters to have a much larger effect upon the flow through one cartridge than the other, for example, the effect of capillary force. Therefore, if experimental functions like (13) and (14) can be found which are independent, then by measuring H_1 and H_2 it will be possible to predict q_g and q_L .

If no mass transfer is assumed to occur between the phases, by continuity the mass flowrates of each phase are equal for both cartridges,

$$(\dot{m}_L)_1 = (\dot{m}_L)_2 \quad (15)$$

$$(\dot{m}_g)_1 = (\dot{m}_g)_2 \quad (16)$$

Since the liquid phase is incompressible the volumetric flowrates through each cartridge are also equal for the liquid, but since the gas is compressible this is not true for the gas.

$$(q_L)_1 = (q_L)_2 \quad (17)$$

$$(q_g)_1 \neq (q_g)_2 \quad (18)$$

In order to calibrate the two porous cartridges for use as a flowmeter

it would be convenient to have a volumetric flowrate for each phase that could be considered the average through both cartridges. If the temperature is essentially constant throughout both cartridges, the volumetric gas flowrate is a function of the mass flowrate and the instantaneous pressure and in terms of the equation of state for an ideal gas, reduces to

$$q_g = \frac{\dot{m}_g}{\rho_g} = \frac{\dot{m}_g R T}{P} \quad (19)$$

where R is the gas constant, T is the absolute temperature and P is the absolute pressure. Since the pressure between the two cartridges, P'' , as shown in Figure 2, may be related to each cartridge by the pressure gradient for that cartridge, the quantity \dot{m}_g/P'' will be taken to be proportional to the volumetric gas flowrate between the two cartridges.

Figure 3a shows hypothetical experimental data which would be determined by measuring flowrates of each phase and the corresponding pressure gradients across each cartridge. If data of this type can be found and shown to be reproducible, it would uphold the hypothesis of unique functional relationship among the pressure gradient and the flowrates of the liquid and the gas. From the graphs shown in Figure 3a the idealized calibration curves shown in Figure 3b may

be drawn. If the curves of Figure 3b have large enough separation, then they may be used to determine flowrates of the liquid and gas by measuring the pressure gradients across each cartridge and the temperature and pressure of the two-phase mixture. The determining of the exact shape of the curves discussed and the requirements for the desired separation in those of Figure 3b is left to another section.

III. EXPERIMENTAL APPARATUS

Test Section

The test section is defined to be the flow channel containing the porous cartridges, the gas injector and the pressure and temperature measurement locations. Figure 4 is an assembly drawing of the test section. Plexiglas was chosen as the material for the test section for its transparency and relative ease of machining and joining. The channel was designed in five sections bolted together at flanges with rubber gaskets making a seal between the flanges. This design was used to simplify the changing of the porous cartridges. The two end sections are 18 inches long and connect to the flexible piping of the test bench. The rest of the test section is made up of three, 3-1/2 inch long, cartridges, two of which contain porous material and the third to serve as a spacer between the two porous cartridges. The gas injector is located 12-1/2 inches upstream from cartridge No. 1.

The channel was constructed using 2" I.D. X 2-1/2" O. D. circular plexiglas stock for the flow tubes and 1/2 inch flat plexiglas plate for the flanges. The tubular sections were cut to length

and the ends machined flat. Then the flanges were machined with a shoulder for the circular sections to seat against. With this type of machined fit it was possible to obtain strong joints using FP-1 solvent for welding plexiglas to plexiglas.

A hollow annulus of plexiglas was machined so that it fit tightly around the 2-1/2 O.D. tube to form the gas injector. Six equally spaced holes 0.040 inch in diameter were drilled radially in the tube before the injector was slipped into place and welded with FP-1. The injector was also drilled and tapped to receive a 1/4 NPT brass fitting for connection to the gas piping from the test bench.

The pressure taps used were standard 1/4 NPT air line brass fittings with an inside diameter of 5/16 inch at the measuring end. After the flow channel was drilled and tapped to receive these fittings, the ends of the fittings were ground down so that they fitted flush with the inside wall of the flow channel.

To provide for monitoring of temperature in the test section, a copper-constantan thermocouple was placed between the two porous cartridges. Number 24 gage thermocouple wire was used and the junction made using lead solder. The leads were run out at a flange between the rubber gaskets to a Leeds and Northrup direct reading potentiometer.

Porous Cartridges

Porous cartridges were tested which were made up from several sizes of round glass beads and an Ottawa sand. The cartridges were formed by clamping copper screen between the rubber gaskets at a flange joint at one end of one of the plexiglas cartridges and then filling it with beads or sand. The cartridges were slightly over filled to insure a close packing. Next, a copper screen was placed over the open end and clamped between the flanges at that joint. In this way the screen was under tension due to the compression of the gaskets and the granular material kept tightly packed. In order to identify the cartridges being tested and direction of flow with respect to gravity, each configuration of the test section was given a number which appears on all data sheets and graphs. A typical designation would be "Configuration II-0°", where Configuration II refers to a particular combination of two porous cartridges with given dimensions and pore sizes and 0° refers to the angle between the flow direction and the gravity vector. Figures 5, 6, 7, and 8 are schematic drawings showing the dimensions, grain size, location of pressure and temperature measurements, and the order in which the fluids pass through the two cartridges for Configurations I, II, III, and IV, respectively. The flow passes through cartridge No. 1 and then through No. 2

in all cases. In Configuration III, cartridge No. 1 was reduced to two layers of 60 mesh copper screen. This was done in an effort to obtain small pore sizes and still have the head loss across this element relatively small. The retainer screen sizes were as follows: for the glass beads of 0.165 inch and 0.118 inch average diameter, No. 8 mesh screen was used and for all of the smaller grain sizes No. 60 mesh screen was used. The gradation of the glass beads is given in Table I. The Ottawa sand used was that part of A.S.T.M. designation C-109 which was retained on No. 60 mesh screen.

Supporting Test Equipment

Figure 9 is a schematic diagram of the test section along with the liquid recirculation and metering system and the gas supply and metering system. A pressure regulator was attached to the laboratory compressed air supply so that a constant air pressure might be supplied to the gas flow meters. Two Fisher & Porter variable area type flowmeters were used to measure the flowrate of air. The smaller one had a capacity of from 0.030 cfm to 0.380 cfm of air at 70^o F and 14.7 psia and the other a capacity of from 0.268 cfm to 3.35 cfm of air at 70^oF and 14.7 psia. In order to determine the air flowrate when the conditions were different from 70^oF and 14.7 psia, the air temperature and pressure were measured at the exit of each meter. A needle valve between the

gas flowmeters and the gas injector was used to control the air flowrate. The water used as the liquid phase in the tests was recirculated by a centrifugal pump. Control of the liquid flowrate was accomplished by restricting the flow with a 1-1/2 inch globe valve. A Rotameter brand variable area flowmeter with a capacity of 0.8 gpm to 8.5 gpm of water was used to measure the liquid flowrate. A metal tank of approximately twelve gallons capacity served as a liquid holding tank and a phase separator. The air entrained in the test section was allowed to escape from the free liquid surface as the liquid decelerated upon entering the tank. Since the electric motor and the liquid pump were mounted on a common metal frame, the liquid gained heat from the motor and its temperature increased with time. Also, the viscous losses in the fluids were transformed into heat and caused a rise in liquid temperature. In order to keep the inlet air and the liquid at approximately the same temperature and also to establish thermal equilibrium sooner, a small flow of cool water was added to the liquid holding tank and a corresponding amount of water from the tank overflowed to drain. This arrangement resulted in a liquid equilibrium temperature between 80 and 85^oF with the inlet air temperature being approximately 78^oF.

The gage pressure and pressure differentials in the test section

were measured with U-tube manometers. The lines from the pressure taps on the channel were filled with water and connected to the manometer tubes which were half filled with mercury or carbon tetrachloride with water filling the remainder of the tube. Mercury was used in all of the manometers except one which used carbon tetrachloride in order to have more sensitivity to small pressure differentials. The manometers built for this investigation used 40 inch glass tubes mounted vertically on waterproof cross section paper which had ten increments per inch. Therefore, the maximum pressure differential that could be measured on one mercury manometer was 40 inches of mercury and the levels read to the tenth of an inch and estimated to the hundredth of an inch.

In order to conveniently mount the test section and the supporting test equipment, a combination work bench and mounting frame was constructed of wood. Figure 10 is a photograph of the test bench showing the manometer board on the left, the vertically mounted flowmeters, and the test section in operation on the right hand end. The liquid pump and holding tank were mounted in the test bench beneath the work table. The test section was mounted on the end of the work bench so that it could be rotated about an axis perpendicular to the flow axis. This provision was made in order to study the effects of varying the direction of flow with respect to gravity.

In this investigation only angles of zero and one hundred and eighty degrees were studied, but other angular orientations between these extremes are possible with the equipment. Flexible rubber hose of 1 inch inside diameter was used to connect the liquid flowmeter to the inlet of the test section and from the outlet of the test section to the liquid holding tank.

IV. EXPERIMENTAL PROCEDURE

The objective of the experiments described in this chapter was to determine the effect that two independent variables, the flowrate of the gas and of the liquid in a two-phase flow through two porous cartridges, have upon two dependent variables, the pressure gradient across each of the two porous cartridges of the test section. In order to accomplish this experimentally, it was necessary to hold one of the independent variables constant while varying the other and measuring the two dependent variables. The accurate measurement of the mass flowrate of air being injected required that the pressure and temperature of the air at the exit of each Fisher and Porter variable area flowmeter be measured. The larger capacity air flowmeter uses a sharp-edged float and therefore viscosity has little effect upon its calibration but the compressibility of the air must be considered. The smaller meter uses a steel ball as a float and its calibration is effected by viscosity and compressibility. The Rotameter brand variable area flowmeter used to measure the water flowrate also uses a sharp-edged float. This fact along with the negligible compressibility of water causes the

calibration of this meter for water flowrate to be independent of pressure and temperature, within reasonable limits. Therefore, because of the nature of the flow measurement for each phase the method of testing was to establish a given liquid flowrate and to vary gas flowrate in regular increments while holding the liquid flowrate constant by manipulating the control valve.

In general, the tests were run starting with the lowest liquid flowrate practical and zero air flow. The liquid flowrate was held constant as the air flow was increased from zero in suitable increments. At each point of operation the pressure differential across each porous cartridge, the gage pressure and temperature between the cartridges, and the gas and liquid flowrates were measured. As the air flowrate was increased, the pressure differentials and the gage pressure in the test section began to fluctuate. This fluctuation seemed to be caused partly by the unstable nature of the two-phase flow and partly by the arrangement of the piping leading from the test section to the liquid holding tank. The maximum air flowrate investigated was that which caused these fluctuations to become so large that reliable data could not be taken with the existing equipment. The maximum liquid rate was limited by the pressure differential across one cartridge becoming too large to be measured with one mercury manometer.

When the system fluctuations were small the manometer readings were averaged by eye and recorded. However, when the variations became so large that reliable readings could not be made in this manner, a mechanical calculator was used to obtain an average reading. The person taking data would glance quickly at the manometer level and then look away and either read the level to an assistant who entered it into the calculator or the reader would enter the number himself. As each successive reading was taken a running total was kept and after a number of readings were taken the average was calculated. This average reading was then recorded on the data sheet.

V. EXPERIMENTAL RESULTS

General Results

The primary purpose of this investigation was to determine the feasibility of using porous cartridges to meter two-phase flow. In an effort to accomplish this and to establish the necessary requirements for success of such a scheme, four separate sets of porous cartridges were assembled and tested in the laboratory. These were termed Configuration I, II, III, and IV and were described in chapter III. Although good data were obtained from Configuration I, II, and IV, that of Configuration III proved to be erratic. This was probably caused by the difficulty of measuring the small pressure drop across the screen used as a substitute for cartridge No. 1. The experimental curves obtained from Configurations I and II do not have the proper characteristics to demonstrate the flowmeter principle, but it is felt that those obtained from Configuration IV do have the correct form. In the next section, data from Configuration II and IV will be presented for comparison. The operation of Configuration I was similar to that of Configuration II, therefore no data from Configuration I is included.

Presentation of Data

The data presented in this thesis is plotted using parameters which are suggested by the form of Darcy's equation even though Darcy's law does not hold for the range of flows which were studied. Since only air and water flows were studied and the operating temperatures were approximately the same for all tests, nondimensional groups such as Reynolds number were not used in plotting the data.

Define the quantity H to be the change in static pressure across a porous cartridge divided by the length of the porous material,

$$H = \frac{\Delta p}{L}$$

and let the subscripts 1 and 2 refer to cartridges No. 1 and No. 2 respectively. The units of H used in this study are psi per inch. The quantity H/μ_L was plotted as the dependent variable of the experimental data, where μ_L is the viscosity of the liquid phase in lb-sec/ft². The independent variables used in plotting the experimental data were the volumetric flowrate of the liquid, q_L , in gpm and the quantity q_g/p'' where q_g is the volumetric flowrate of the gas when measured at 70° F and 14.7 psia and p'' is the absolute pressure between cartridges No. 1 and No. 2. The units of q_g/p''

are scfm/psia. Figure 11 is a typical plot of experimental data which was taken for cartridge No. 1 for downward flow through Configuration II. The ordinate used is the quantity H_1/μ_L multiplied by 10^{-4} and the abscissa is q_g/p'' multiplied by 10^2 with the liquid flowrate in gpm as a parameter. The liquid flowrates corresponding to the symbols used are given on the page facing Figure 11 and are the same for Figures 11 through 24. The data plotted on Figure 12 was taken for cartridge No. 2 for downward flow through Configuration II. The data for Figures 11 and 12 were taken simultaneously. Figure 13 is a plot of $H_1/\mu_L \times 10^{-4}$ versus $H_2/\mu_L \times 10^{-4}$ with q_L as a parameter for downward flow through Configuration II. This plot represents the same data as Figures 11 and 12 combined. Figure 13 is entitled Calibration Data since a plot of this type could be used to determine the liquid flowrate if the values of H_2/μ_L and H_1/μ_L were known and the curves had sufficient separation. The gas flowrate could then be obtained from Figure 11 or 12. The experimental data for upward flow through Configuration II are shown on Figures 14 and 15 with Figure 16 being the calibration data for downward flow, similar to Figure 13.

The data as plotted in Figure 13 and 16 for Configuration II show this particular combination of porous cartridges to be unsuitable for use as a two-phase flowmeter. Since the plots of H_1/μ_L versus

H_2/μ_L for parametric values of liquid flowrate lie almost one on top of the other and in approximately a straight line, these figures show that H_1 and H_2 are not independent functions of the flow parameters for the flow range covered, i.e. one is approximately a constant multiple of the other. This means that the flow through one cartridge is approximately a model of the flow through the other. Under such conditions it will not be possible to predict the flowrates of the two phases since there are an infinite number of combinations of liquid and gaseous flowrates which will produce a given permissible set of H_1 and H_2 .

Figures 17 and 18 are plots of experimental data taken on three different days for downward flow through Configuration IV. This same body of data is shown in the form of calibration curves as Figure 19. Figures 17 and 18 demonstrate the amount of data scatter that was encountered in the tests. The corresponding plots for upward flow are given as Figures 20, 21, and 22. From Figure 19 it may be seen that the curves for different constant q_L values are quite distinct and have the general form of parallel curves. The same form is demonstrated by Figure 22 for upward flow, although the separation is not as well defined.

Comparison of Figure 12 with Figure 19 indicates that there was a basic difference in the flow characteristics between Configuration

II and IV. In Configuration II the porous cartridge with the larger grain size was placed in the No. 1 position in the flow, but in Configuration IV this arrangement was reversed. The effect of this change was to cause a relatively larger expansion of the gaseous phase through cartridge No. 1 in Configuration IV than in Configuration II. With the same set of porous cartridges the liquid Reynolds number (based on grain size) for the smaller grain cartridge would be lower if it were the No. 1 cartridge than if it were the No. 2 cartridge. Also, the liquid Reynolds number for the larger grain cartridge would be larger if it were the No. 2 cartridge than if it were the No. 1 cartridge. Both of these effects are due to the expansion of the gaseous phase and the consequent increase in liquid velocity as the pressure decreases across a porous cartridge. The ratio of the grain size between the two cartridges in Configuration II was about 2:1 and in Configuration IV this same ratio was approximately 16:1. If a liquid Reynolds number is based upon the grain size of the finer grain cartridge and the liquid flow area is decreased by the ratio of liquid flowrate to total average volumetric flowrate, the liquid Reynolds number for 3 gpm liquid rate and an average air flowrate of 0.3 cfm, was calculated to be approximately 700 for Configuration II and approximately 120 for Configuration IV. The effect of capillary pressure was probably responsible for part of the differences in flow

characteristics between Configurations II and IV. The magnitude of this effect may be estimated by the expression,

$$p = \frac{4\sigma}{d}$$

where σ is the surface tension of the liquid-gas interface and d is the average pore size. For the smaller grain size cartridges, the capillary pressure, p , was estimated to be 0.055 inch of mercury for Configuration II and 0.33 inch of mercury for Configuration IV. Therefore, the capillary effect was approximately six times as large in Configuration IV as in Configuration II.

Figure 19 indicates that it would be possible to determine flowrates of a two-phase mixture by measuring the pressure drop across two porous cartridges if the calibration curves are similar to those of Figure 19. With a two-phase mixture flowing through the two cartridges, the pressure drop across each can be measured. Along with a temperature measurement, this determines the quantities H_1 / μ_L and H_2 / μ_L . Using these coordinates, a point is specified on a plot similar to Figure 19 which corresponds to a particular liquid flowrate. Using Figure 19, there would be considerable error in determining q_L , but in principle q_L would be unique for a given H_1 / μ_L and H_2 / μ_L . Once q_L is known, a plot of the form

of Figure 17 or 18 could be used to determine q_g and the flowrate of the two phase mixture would be determined.

Figure 23 is an idealized sketch which is based upon experimental calibration data and extended according to the observed trends of the data. It may be seen that the lines of zero liquid flowrate and zero gas flowrate form the boundaries of an envelope within which all possible operating points are contained. This sketch suggests that the conditions for using two porous cartridges as a two-phase flowmeter successfully are that the lines of $q_g = 0$ and $q_L = 0$ be as widely separated as possible and that operating points be as far away from the "vertex" of the envelope as possible.

Effects of Flow Patterns

Figures 26 and 27 are photographs of the test section in two-phase upward flow. The flow between the gas injector and cartridge No. 1 may be seen in Figure 27. This flow pattern may be termed bubble flow since the liquid phase is continuous and the gas is in bubble form. The effect of the porous cartridges was to break up the bubbles into smaller sizes and to homogenize the flow. This is shown in the photograph on the right side of Figure 26. As the flowrate of air was increased the bubbles leaving cartridge No. 2 began to increase in size due to a recombining of smaller bubbles. As this process increased until the largest bubbles were of the same

order of size as the flow tube, slug flow began. This slug flow was characterized by large variations of pressure and flowrates. No data were taken in the slug flow range.

Figure 28 shows two photographs of the porous cartridges in downward flow. The two-phase flow pattern for downward flow was similar to annular flow in that the liquid tended to flow either down the wall or as small separate streams with the gas phase being continuous. This type of flow occurred throughout the flow ranges over which data was taken. Again the effect of the porous cartridges was to homogenize the flow by breaking the liquid streams into smaller streams and sheets. This may be seen in the photograph on the right side of Figure 28 as the flow passes through cartridge No. 1.

Figures 24 and 25 are plots of experimental data for Configuration IV in which the points of upward and downward flow have been plotted on the same axes. In all of the data presented only static pressure differences have been used with no correction for the differences in the elevation. If a factor of ρg , where ρ is the density of water, were included, the quantity H/μ_L would change by the constant amount 0.212×10^4 for a water temperature of 84°F . However, it is not completely clear whether this is the proper correction since the density of the two-phase mixture and the effect of capillary forces are not known in the porous cartridges. Although some

correction factor needs to be applied to the data as shown by Figures 24 and 25, it may be seen that the flow characteristics for upward and downward flow through the cartridges are similar.

Sources of Error

The primary difficulty in making meaningful comparisons between sets of data and in trying to demonstrate the reproducibility of the calibration data was the loading up of the pores of the small grain porous cartridges with foreign matter. This was observed by the discoloration of the porous material and an increase in pressure drop across the fine grain cartridges after several days of testing. This increase in pressure drop with time was not observed for the larger sizes of glass beads; therefore, it was concluded that this was due to a loading up of the small pores and not a change in flow conditions with time. The principle source of this foreign matter was the liquid pump which had a cast iron casing which rusted due to its being filled with water at all times. The rusting could be observed as a discoloration of the water when the pump was switched on after being off over night. A 60 mesh screen in the liquid line was used to filter out larger particles, but was not successful in removing the small rust particles. A thin wafer of the Ottawa sand was also placed upstream of the test section in an attempt to remove the rust particles, but this was not completely successful either. It was

observed that high flowrates of air and water would flush part of the rust particles out of the cartridges. Therefore, in an effort to obtain similar conditions for all the tests, after a particular cartridge had been in use for a day or two, the procedure was adopted to flush out the cartridges before test was begun. The data indicated a partial reversal of the increased pressure drop effect after this method was used.

The fluctuations of the manometer readings were a source of error, but the use of the averaging technique described in chapter IV held this to a minimum. During the test runs on Configuration IV, a mercury manometer was used to measure the pressure differential across cartridge No. 1, but the pressure differential across cartridge No. 2 was measured with two different manometers. Since the pressure drop across cartridge No. 1 was many times larger than across No. 2, a U-tube manometer using carbon tetrachloride as a fluid was used to measure the pressure drop across cartridge No. 2 when the flowrate was 1.0 and 2.0 gpm. However, for larger values of liquid flowrate the pressure drop was too large to measure in this way and a mercury manometer was used. Due to this shift in types of manometers, there was a change in sensitivity which was probably reflected in the accuracy of the data.

Two different variable area flowmeters were used at various

times to measure inlet liquid flowrate. Due to the ranges of flows studied, both of these meters were usually operated on the lower half of their range which increased their rated error of one and two per cent of the maximum scale reading. Both of the flowmeters used to measure inlet air flowrates were calibrated for one per cent error of the maximum scale reading. The smaller of these was used over its complete range and the larger up to approximately thirty per cent of maximum.

VI. CONCLUSIONS AND RECOMMENDATIONS

Based upon data obtained in the course of this study, it appears that the metering of gas-liquid two-phase flow is feasible for a certain range of flows using as primary elements two porous cartridges. The total flow must pass through each in series and the cartridges must be calibrated for the given gas and liquid over the range intended. Using calibration curves obtained previously, the flowrates of each phase may be determined by measuring the pressures and temperatures in the metering section.

Tests were run only for vertically upward and for vertically downward flow, but the flow characteristics of each were shown to be similar. The principle of metering two-phase flow was demonstrated for flow in either direction by the use of the static pressure difference as an indication of resistance to flow. Although the use of total head drop across a cartridge only involves the addition or subtraction of a constant term to the static pressure difference in single phase flow, in two-phase flow the magnitude of the correction is uncertain. Based upon the properties of the gas and liquid this correction might be a function of flowrates or merely a constant.

If this point could be clarified, there is evidence that the calibration curves could possibly be independent of flow direction.

The first requirement for this metering principle to work is that the flow through each of the cartridges be enough dissimilar that the pressure gradients across each cartridge are independent functions of the flowrates of each phase. This requirement may be satisfied by the flow regimes being different in each as indicated by Reynolds numbers or by a phenomenon such as capillary pressure being important in one cartridge and not the other.

The addition of a reliable particle filter, with a large surface area, to the flow system would improve the reproducibility of the data and would result in a better understanding of the flow characteristics. The silting of the fine grain porous cartridges was a consistent problem in the investigation and the various methods used to combat it were incomplete in their effectiveness.

The use of piezometer rings instead of single openings for pressure taps seems advisable to obtain more fundamental pressure readings. Also, the averaging properties of such a device might eliminate part of the pressure reading fluctuations. If the dimensions of the porous cartridges were adjusted so that the pressure difference across each was approximately the same, an improvement in meter sensitivity would result. This could be

accomplished by making the cartridge which uses the finer grain size shorter and with a larger area than the cartridge made up of the larger grain size. The grain size and flow area determine the flow regime, but the total pressure drop is also a function of the cartridge length.

Table 1. Gradation of Glass Beads

Average bead size	per cent by weight	retained on screen	but passing screen
0.165 in.	90	No. 5	No. 4
0.118 in.	90	No. 8	No. 6
0.060 in.	95	No. 14	No. 12

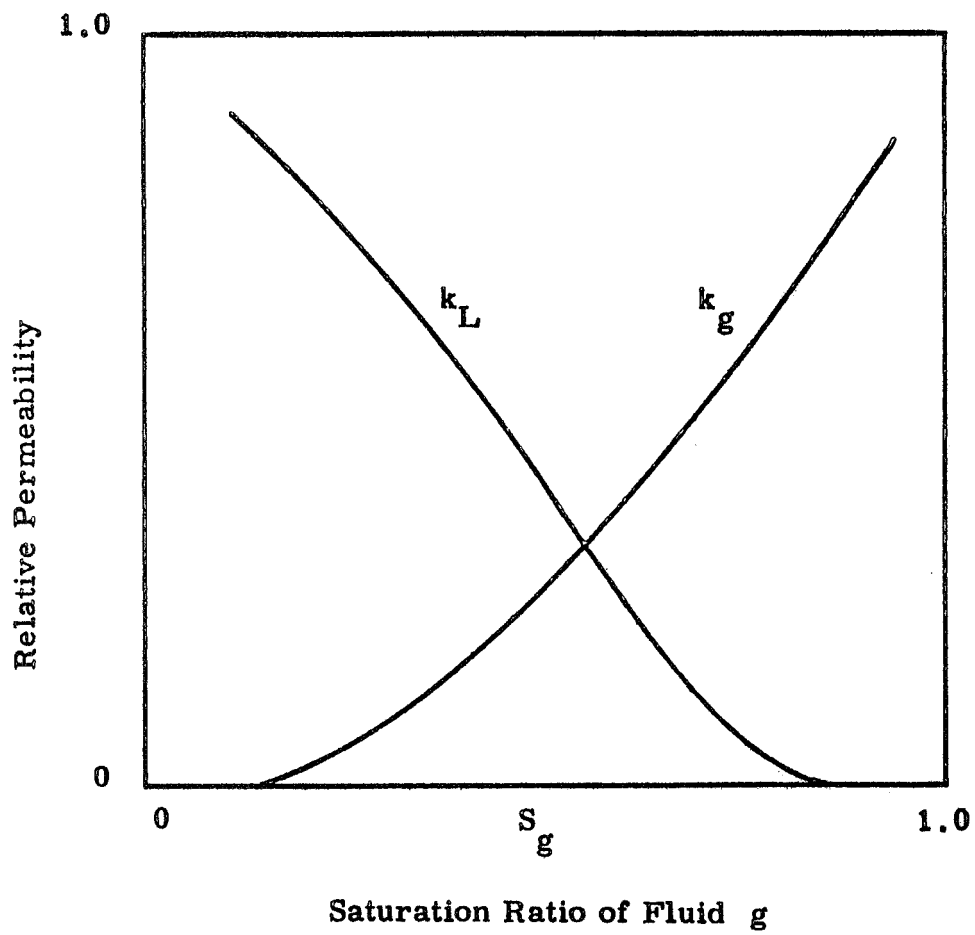


Figure 1. Typical Relative Permeability Curves
[2], [13]

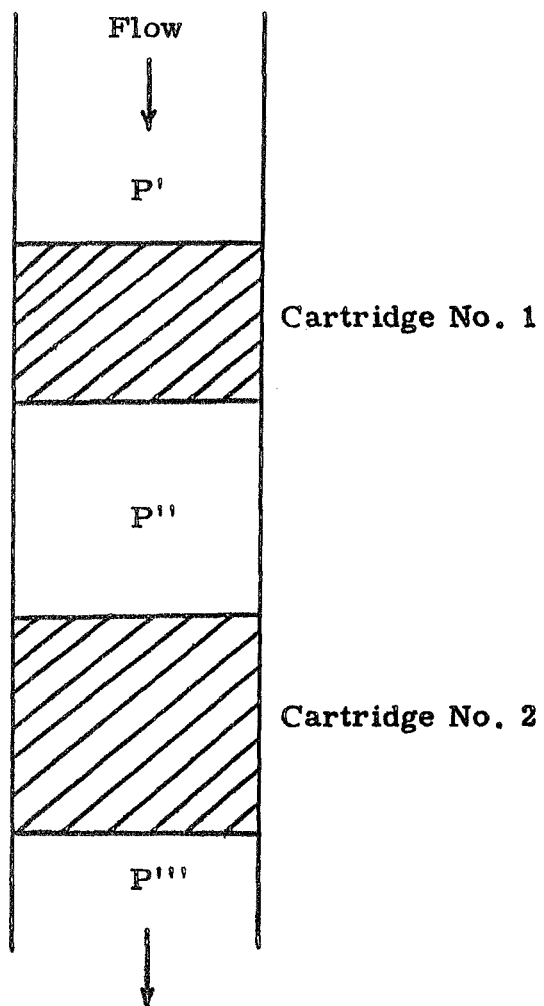


Figure 2. Porous Cartridge Arrangement in Two-Phase Flow Channel

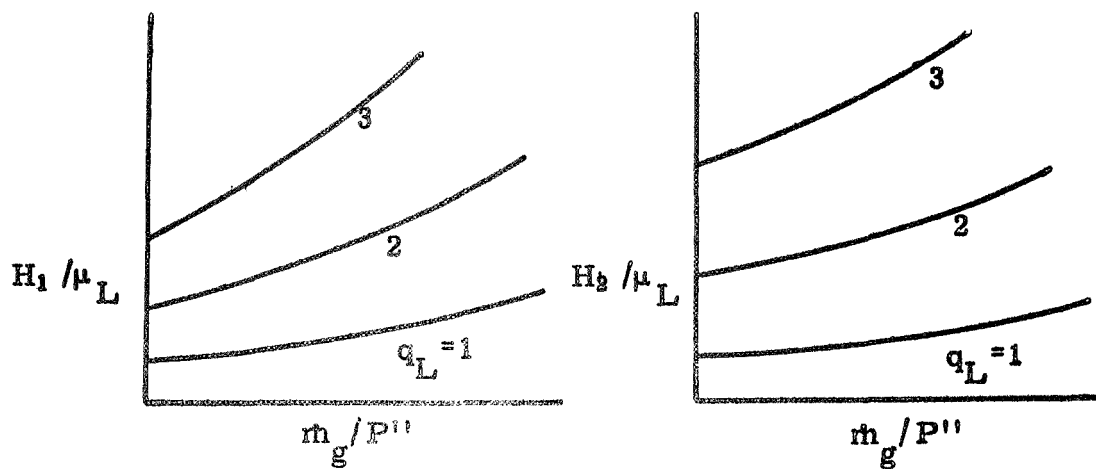


Figure 3a. Hypothetical Experimental Data

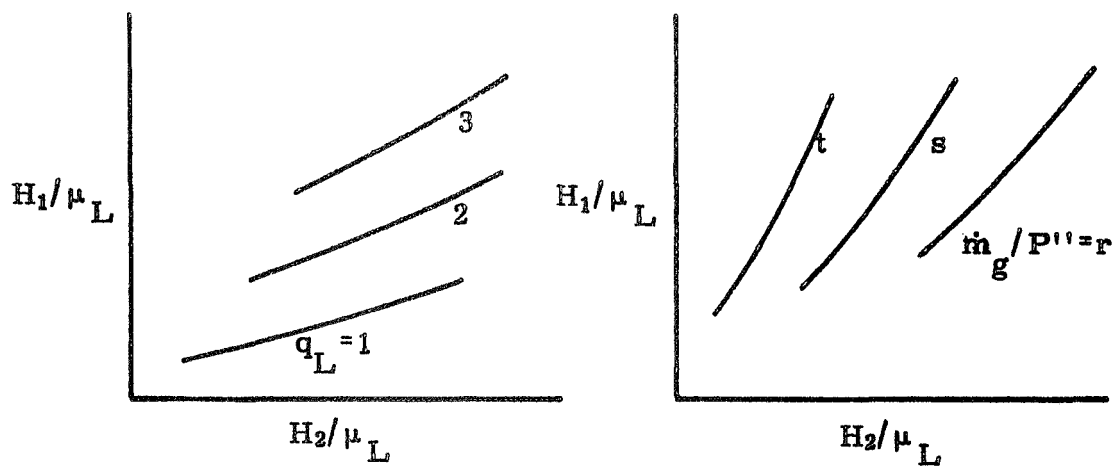


Figure 3b. Hypothetical Calibration Curves

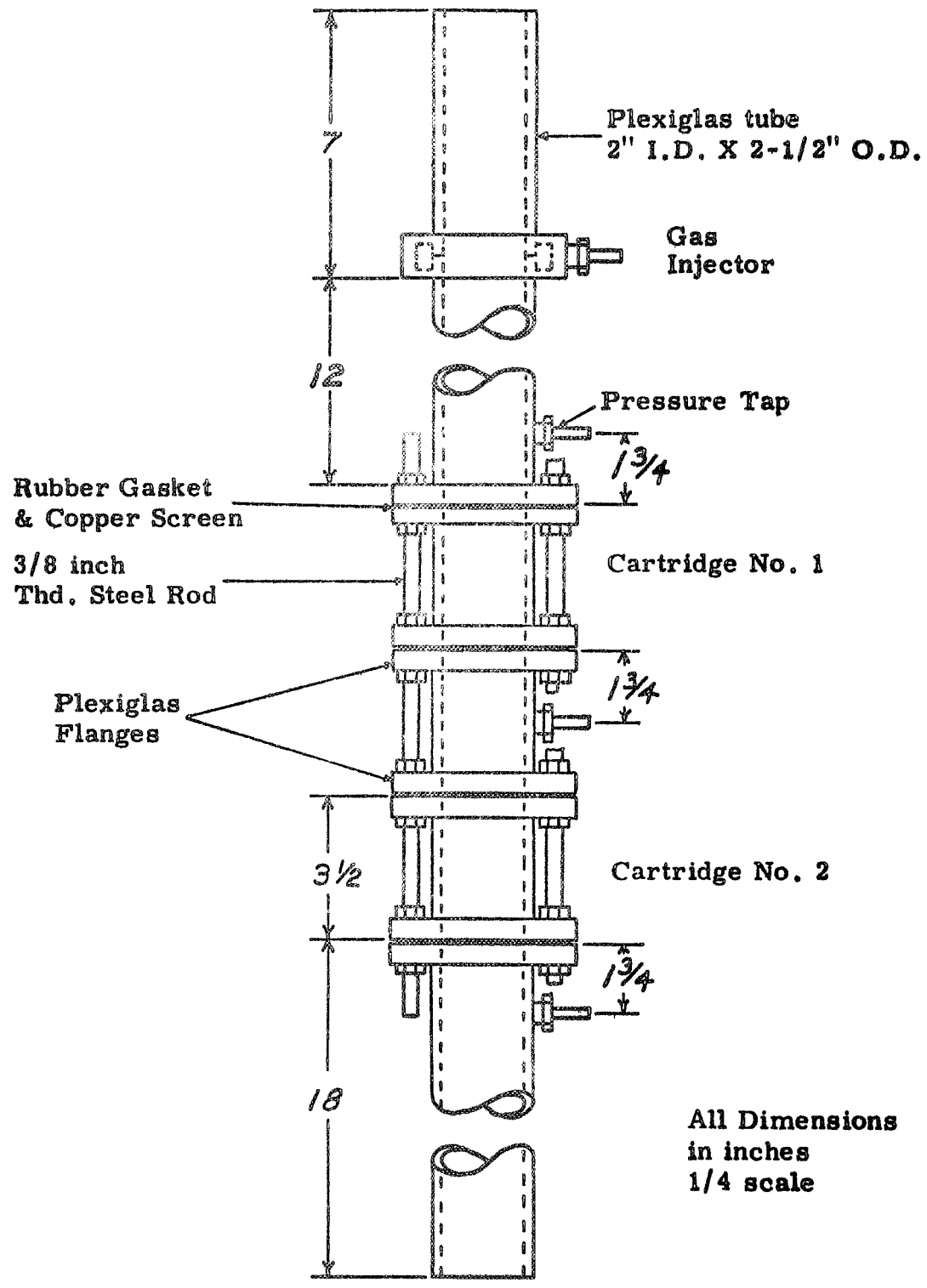


Figure 4. Assembly Drawing of Test Section

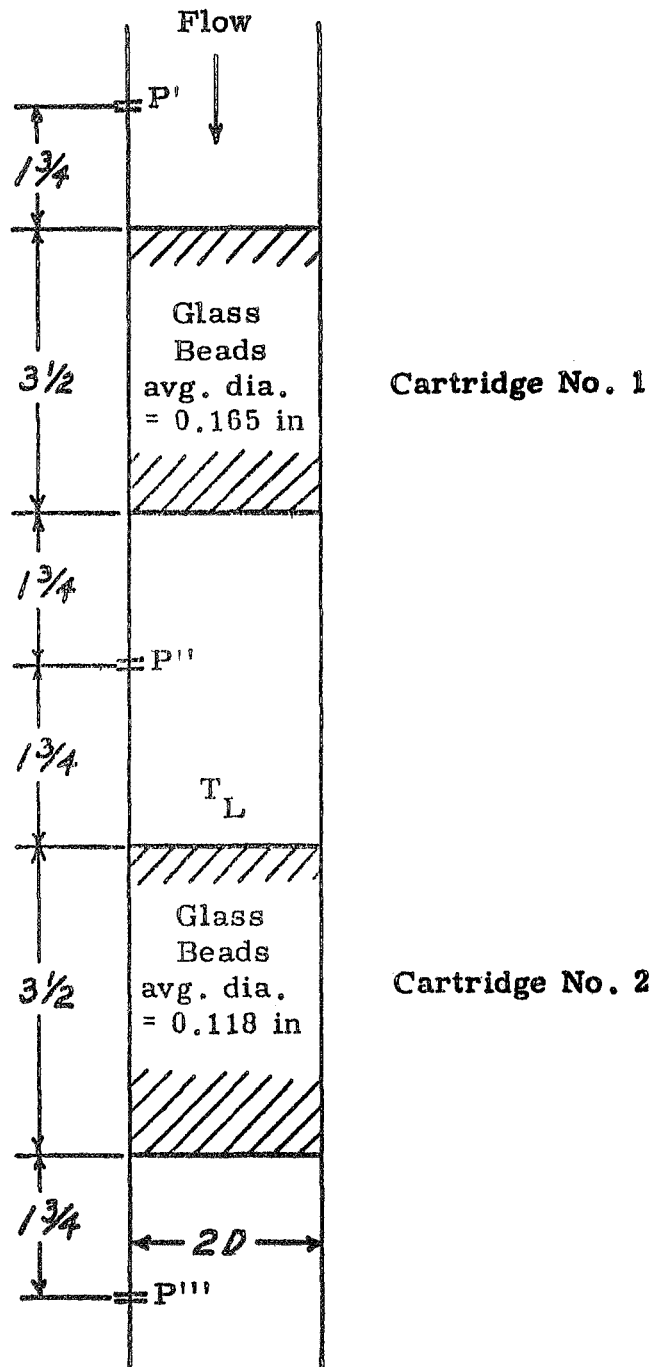


Figure 5. Porous Cartridges - Configuration I

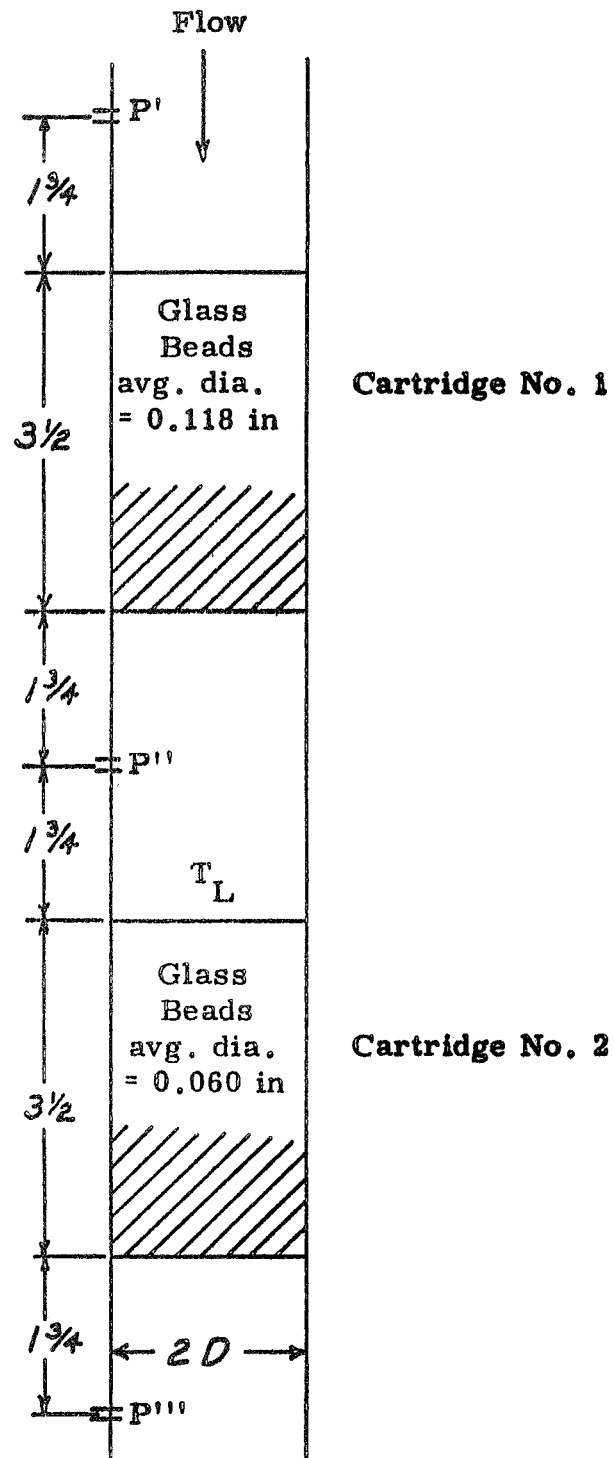


Figure 6. Porous Cartridges - Configuration II

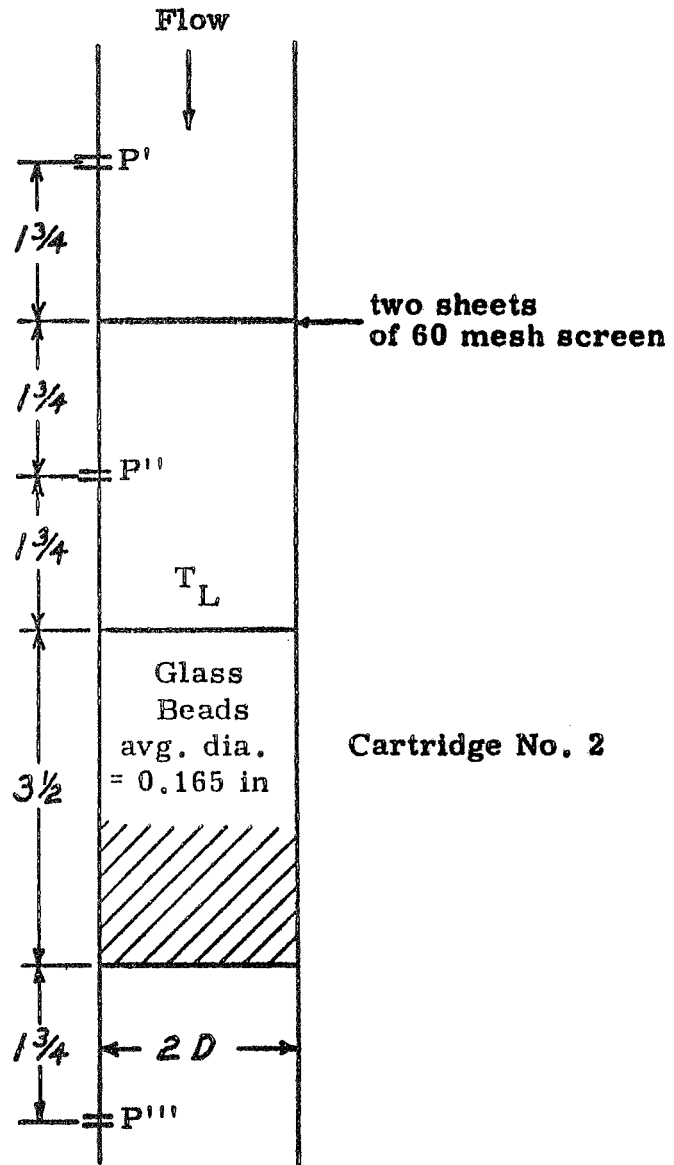


Figure 7. Porous Cartridges - Configuration III

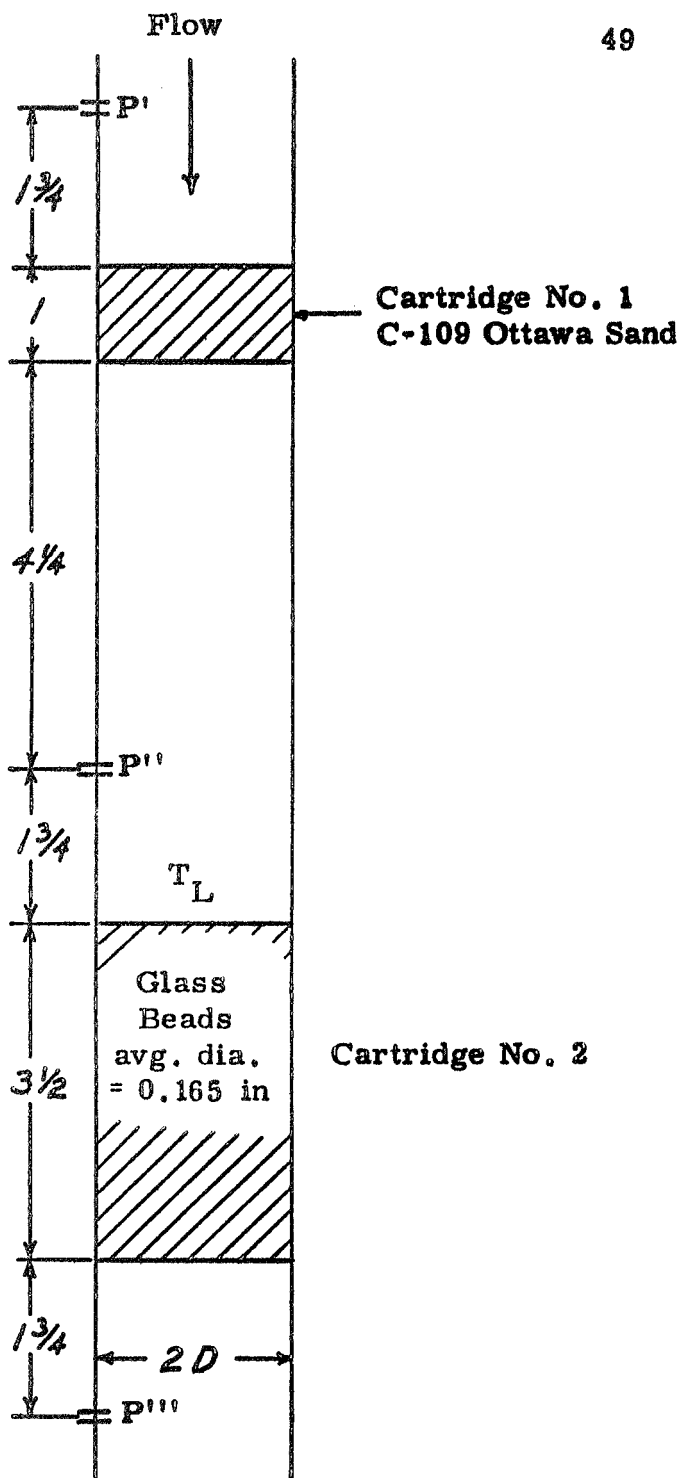


Figure 8. Porous Cartridges - Configuration IV

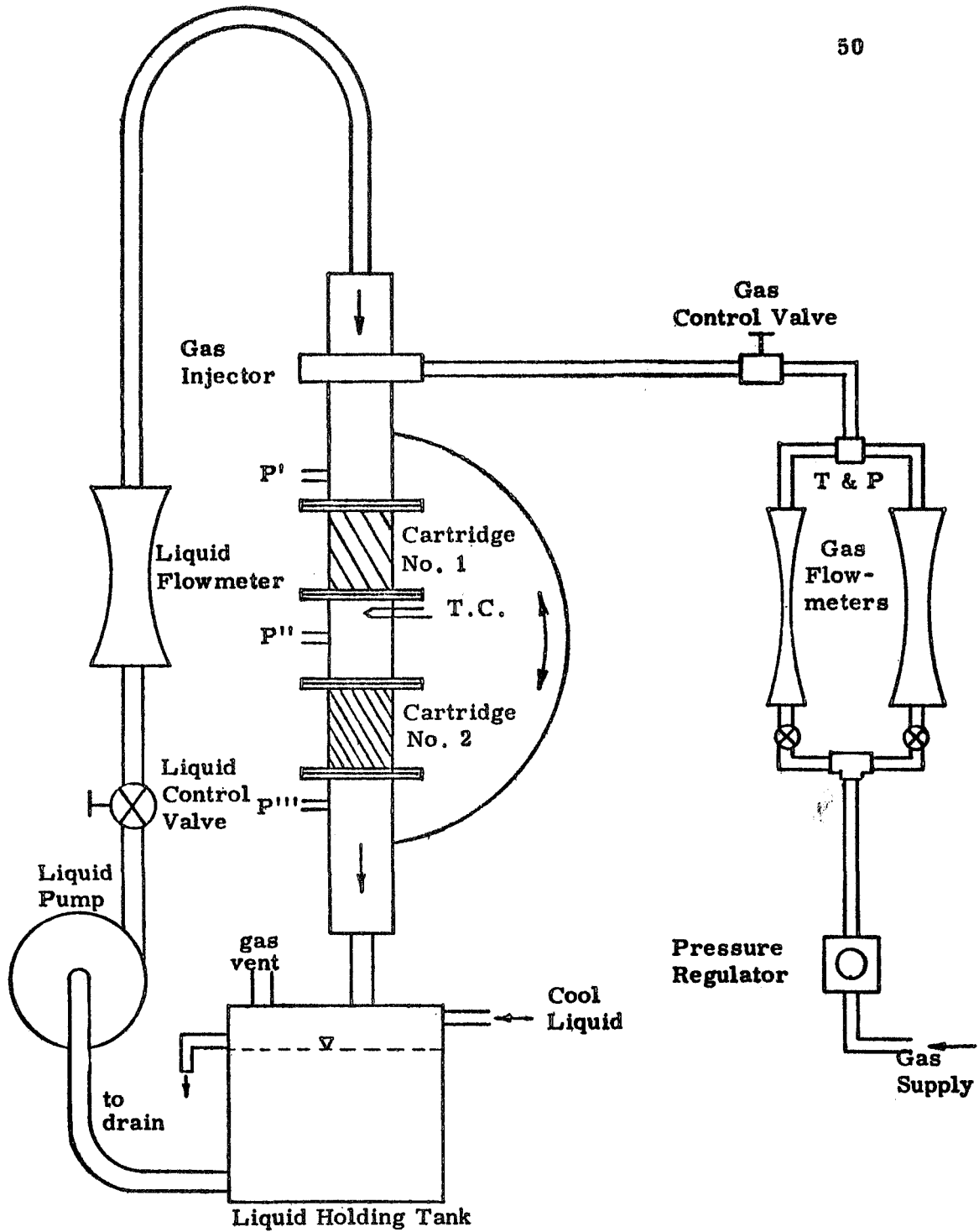


Figure 9.

**Schematic Diagram of Experimental Apparatus for
Two-phase Flowmeter Calibration**

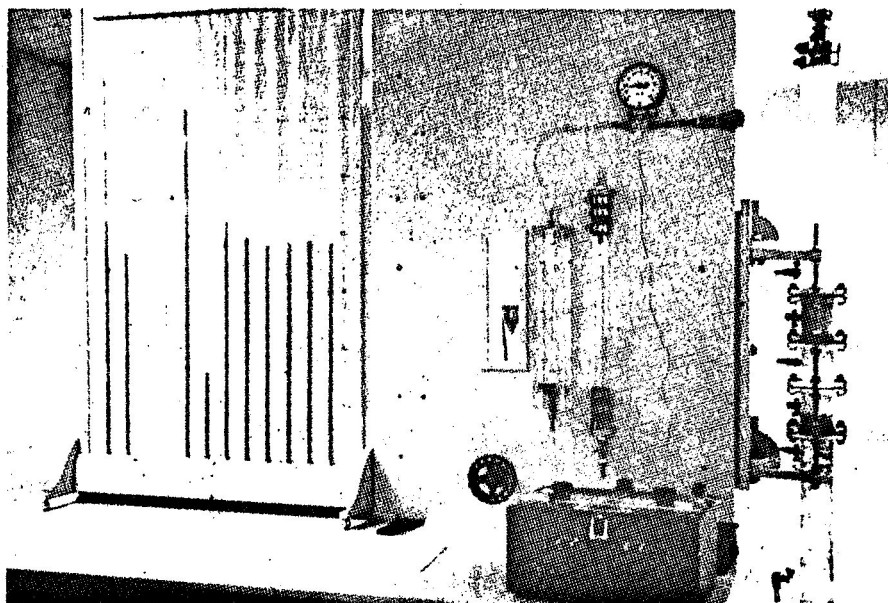


Figure 10. Test Bench

Legend:
The symbols below, representing the given liquid flowrates, apply uniformly to Figures 11 through 25.

∇ $q_L = 1.0$ gpm

\succ $q_L = 2.0$ gpm

\odot $q_L = 3.0$ gpm

\square $q_L = 4.0$ gpm

\triangle $q_L = 5.0$ gpm

\diamond $q_L = 6.0$ gpm

\ddagger $q_L = 7.0$ gpm

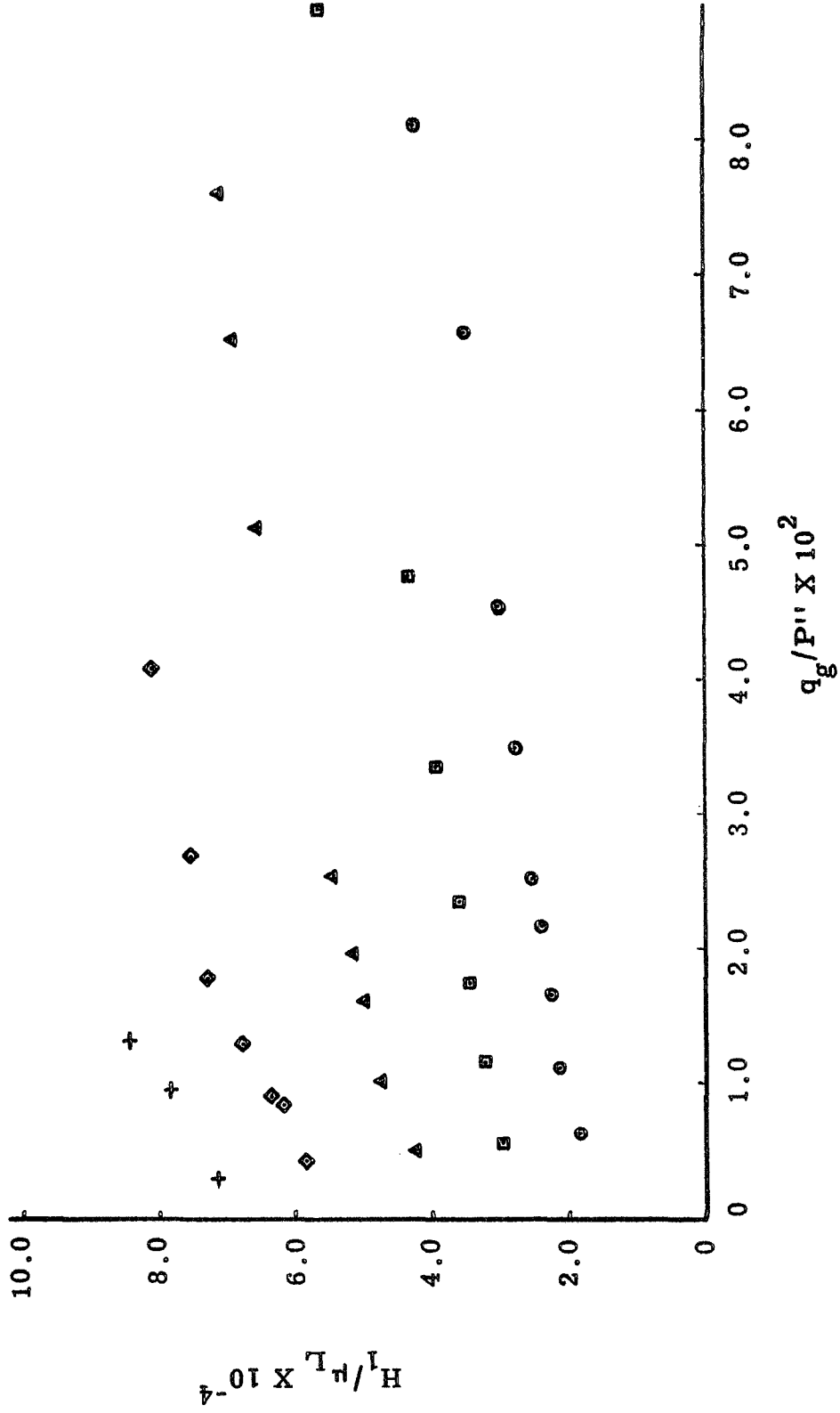


Figure 11. Experimental Data - Configuration II - 0°, Cartridge No. 1

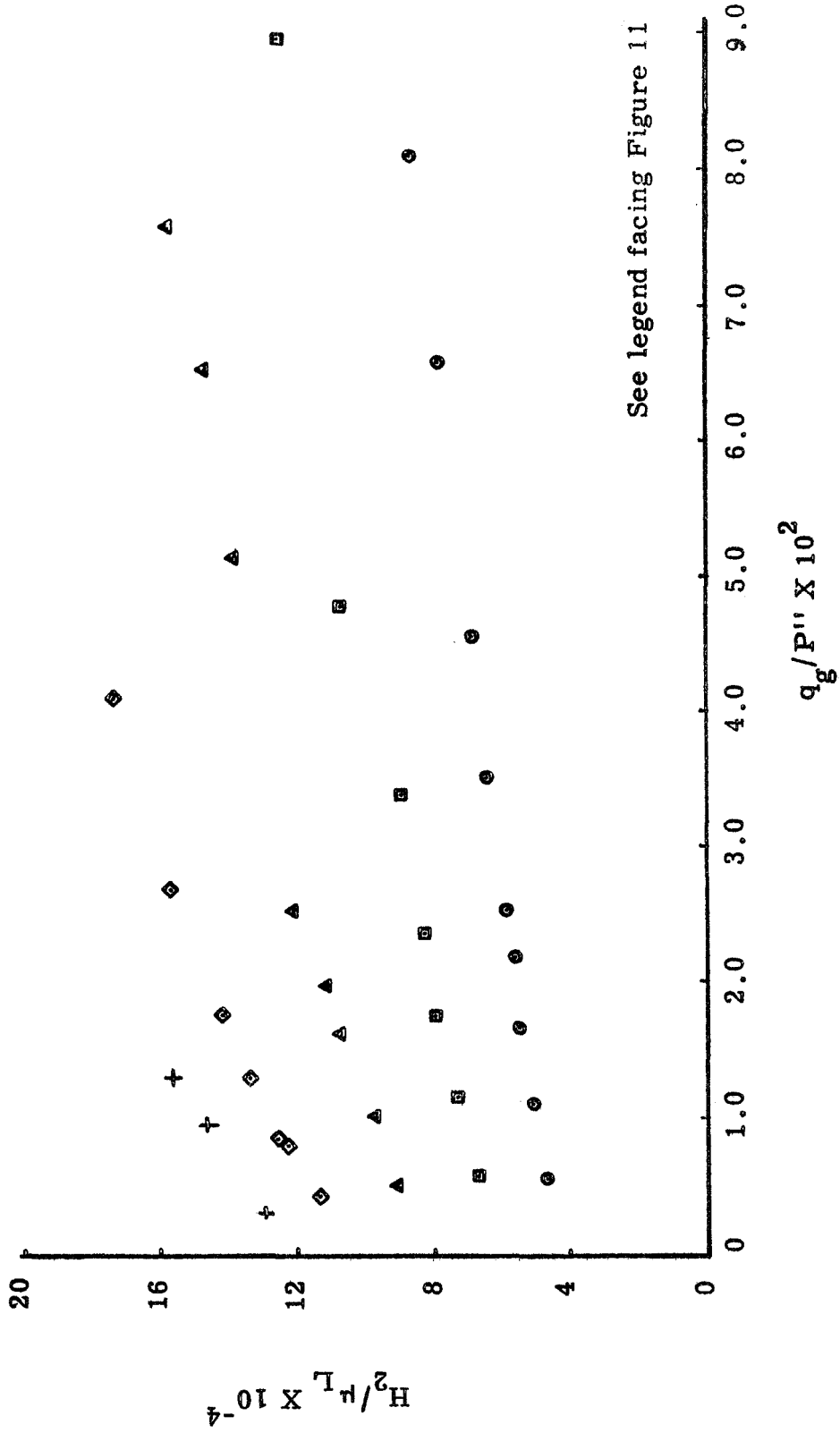


Figure 12. Experimental Data - Configuration II - 0°, Cartridge No. 2

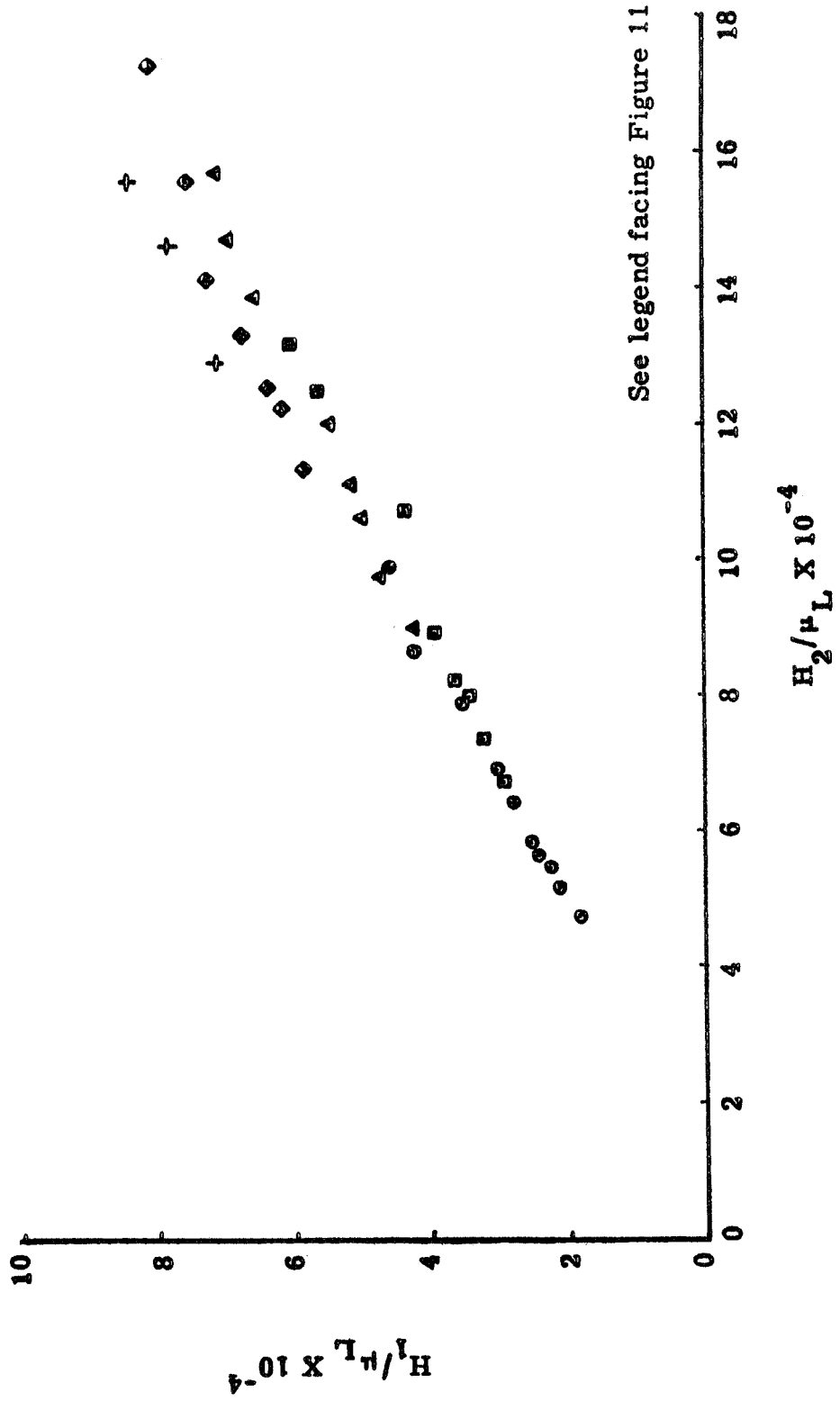
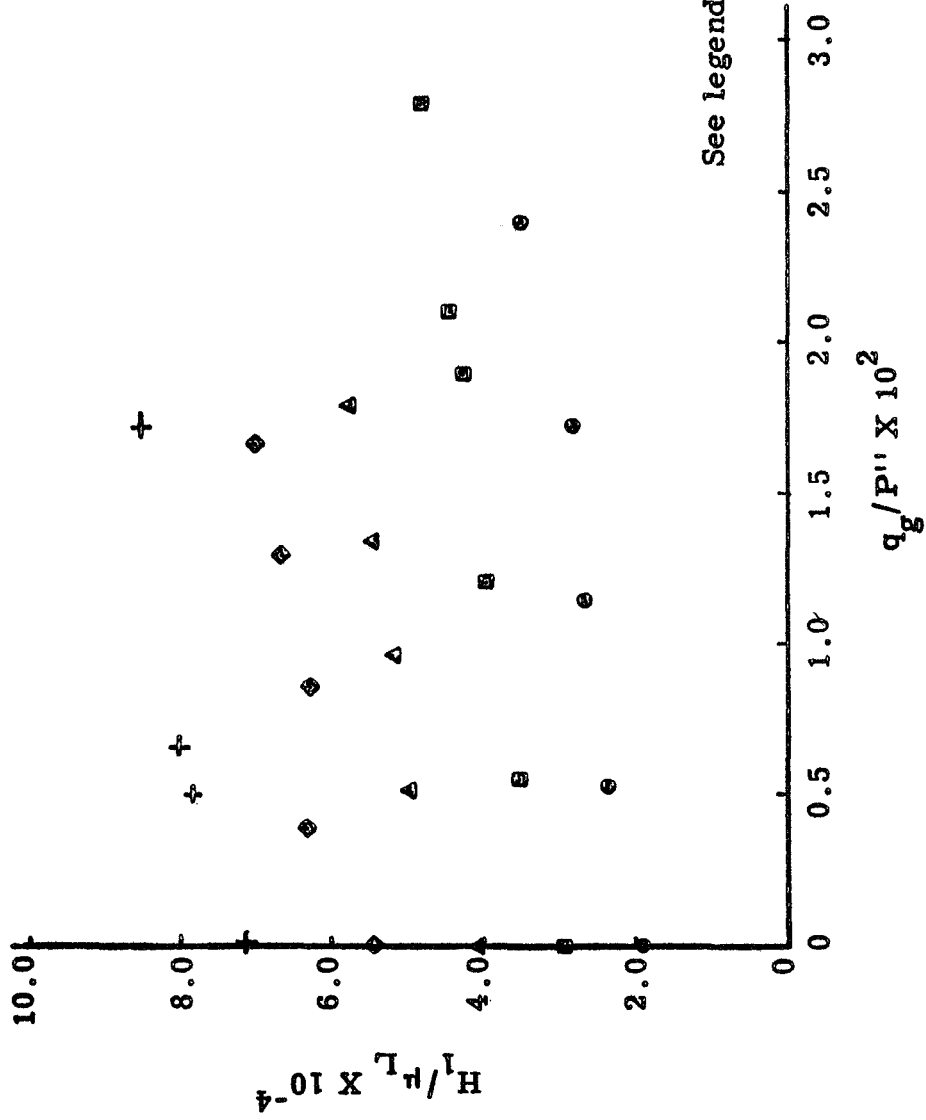
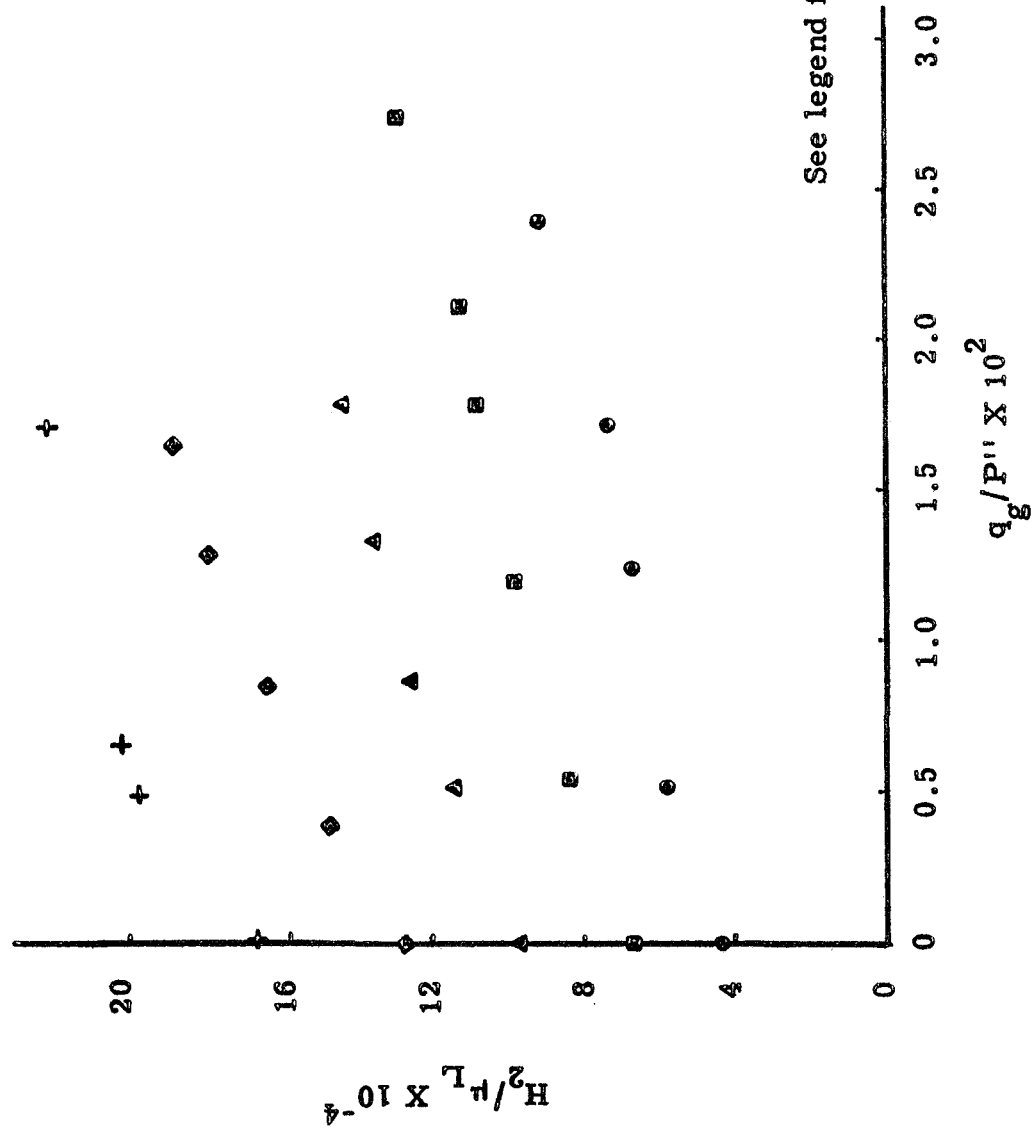


Figure 13. Calibration Data - Configuration II - 0°



See legend facing Figure 11

Figure 14. Experimental Data - Configuration II - 180°, Cartridge No. 1



See legend facing Figure 11

Figure 15. Experimental Data - Configuration II-180°, Cartridge No. 2

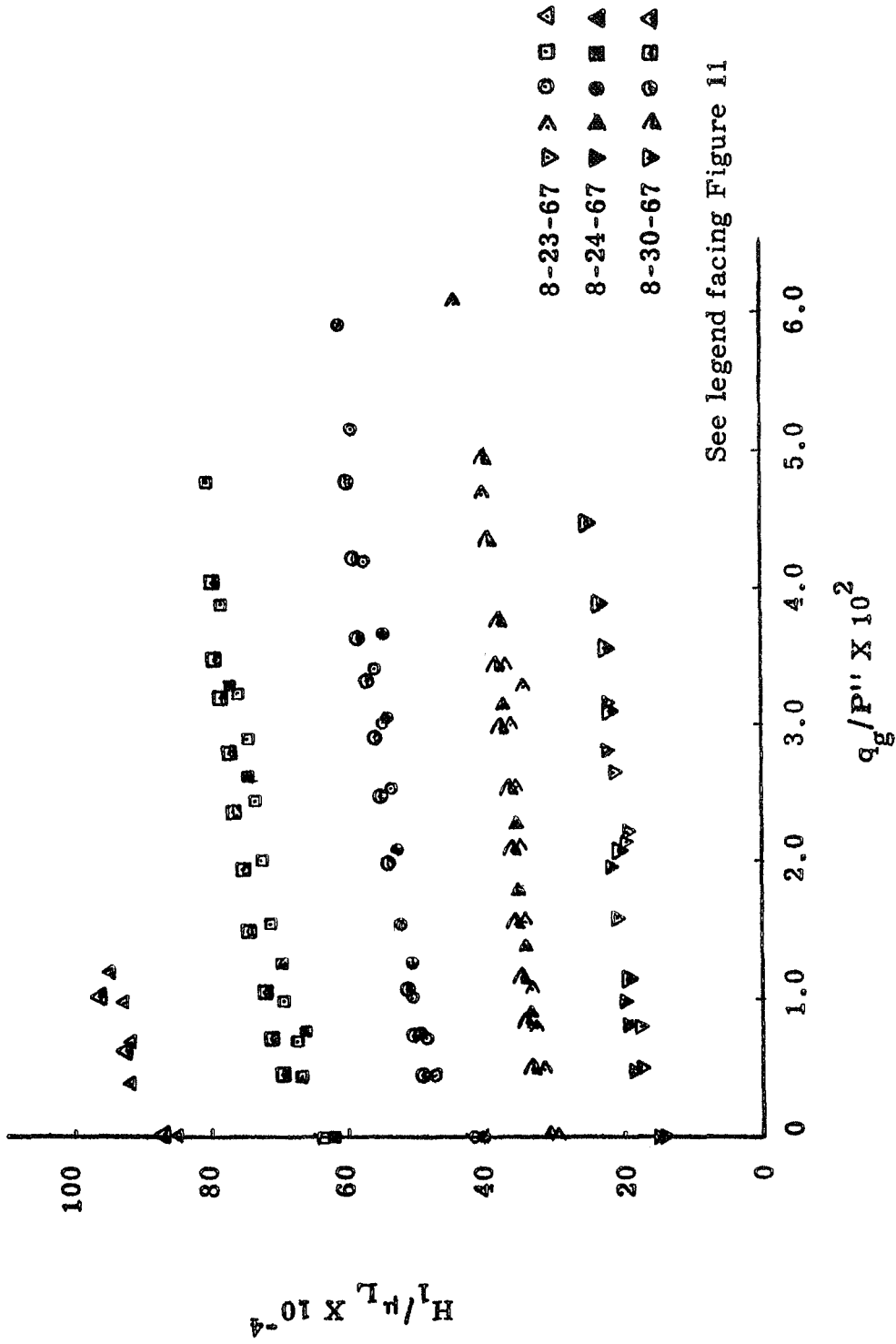


Figure 17. Experimental Data - Configuration IV - 0°, Cartridge No. 1 59

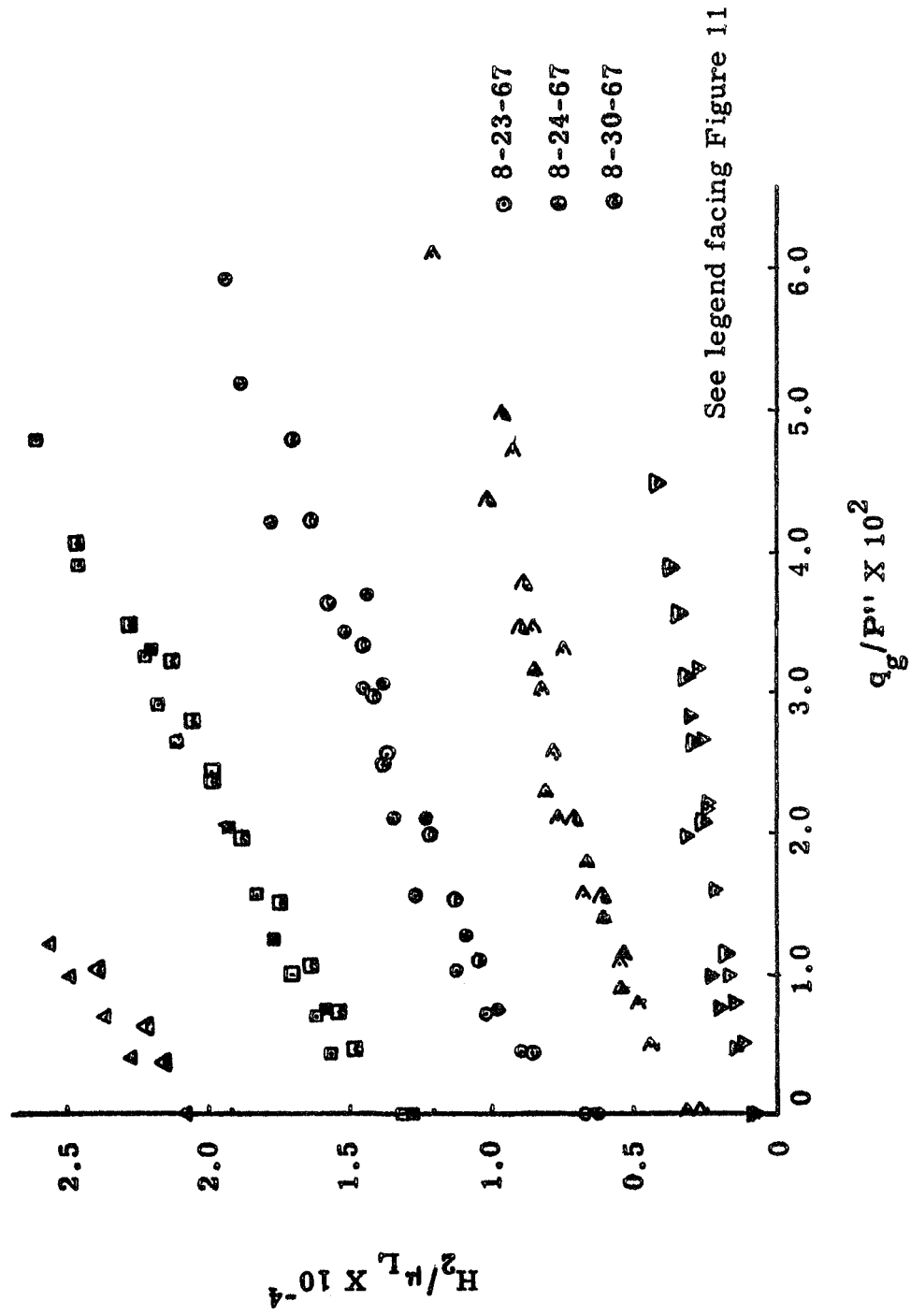


Figure 18. Experimental Data - Configuration IV - 0°, Cartridge No. 2

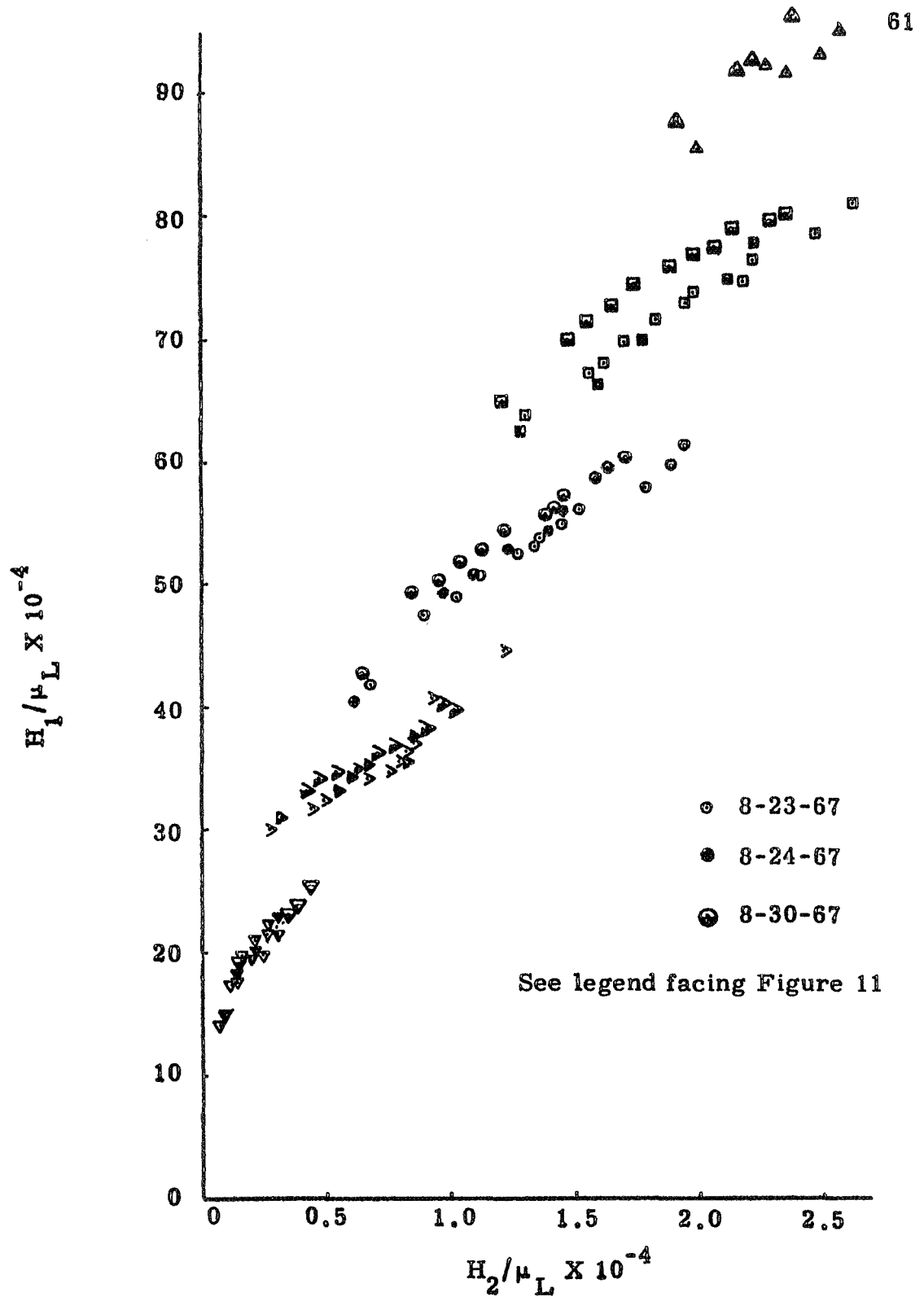
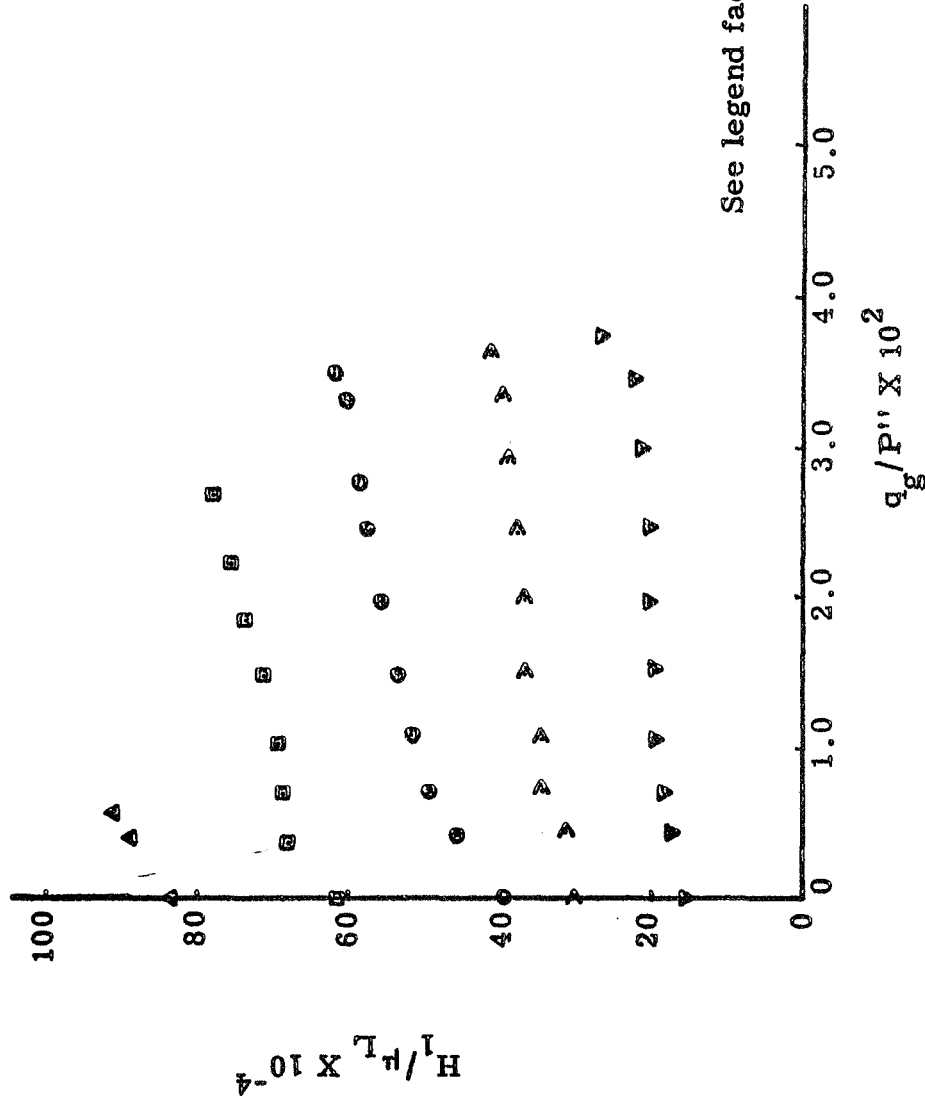


Figure 19. Calibration Data - Configuration IV - 0°



See legend facing Figure 11

Figure 20. Experimental Data - Configuration IV - 180°, Cartridge No. 1

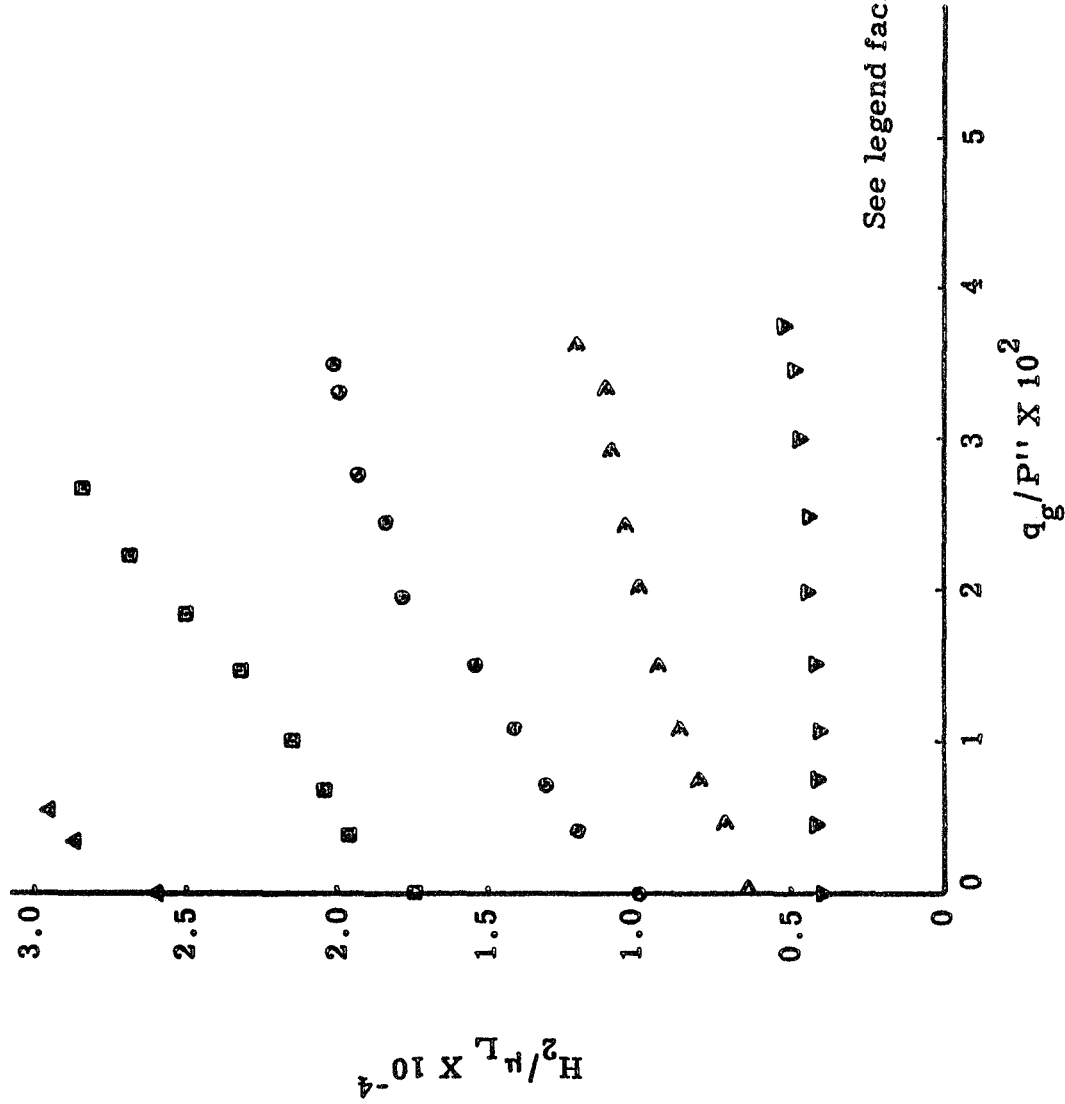


Figure 21. Experimental Data - Configuration IV - 180°, Cartridge No. 2

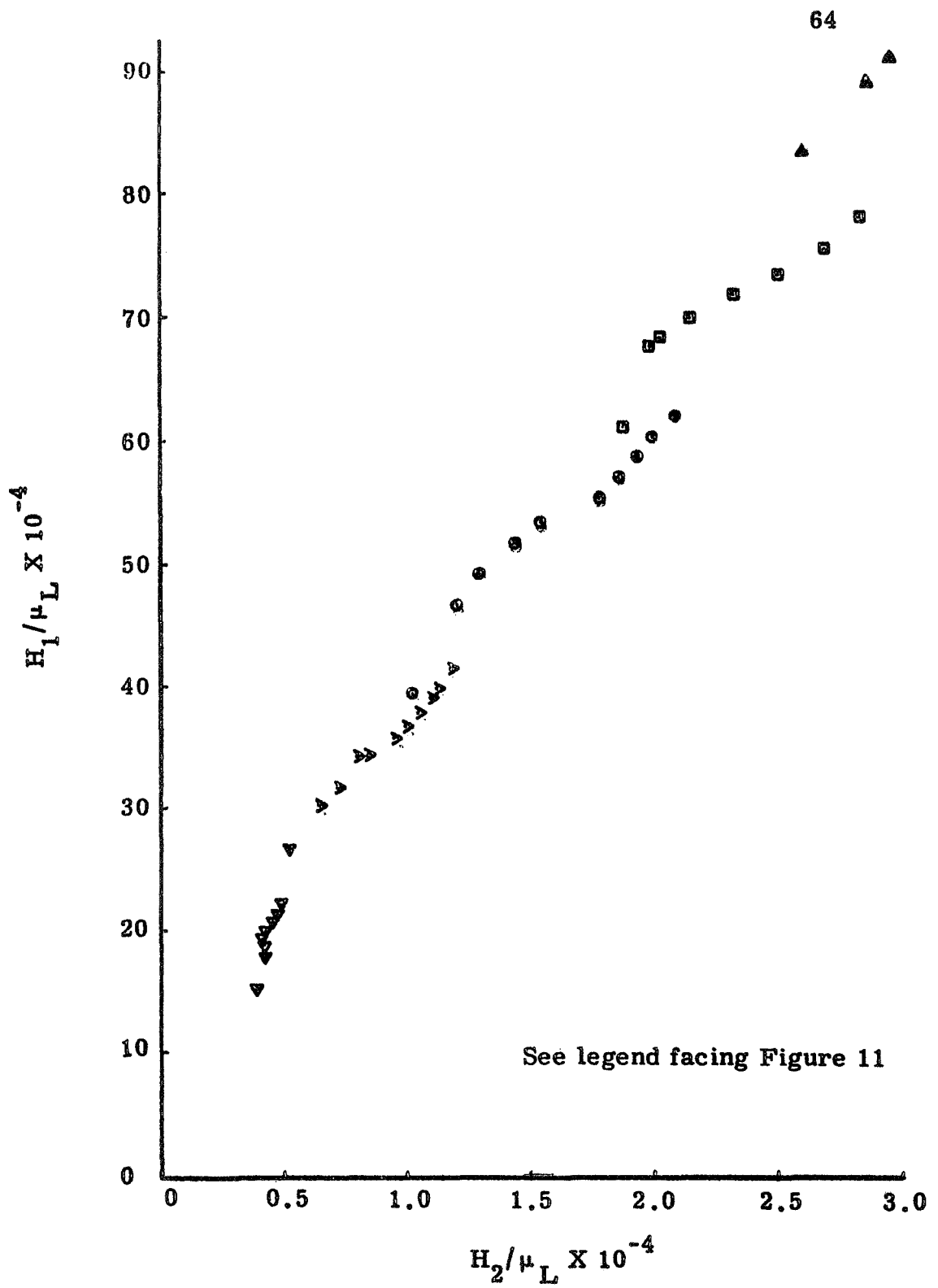


Figure 22. Calibration Data - Configuration IV - 180°

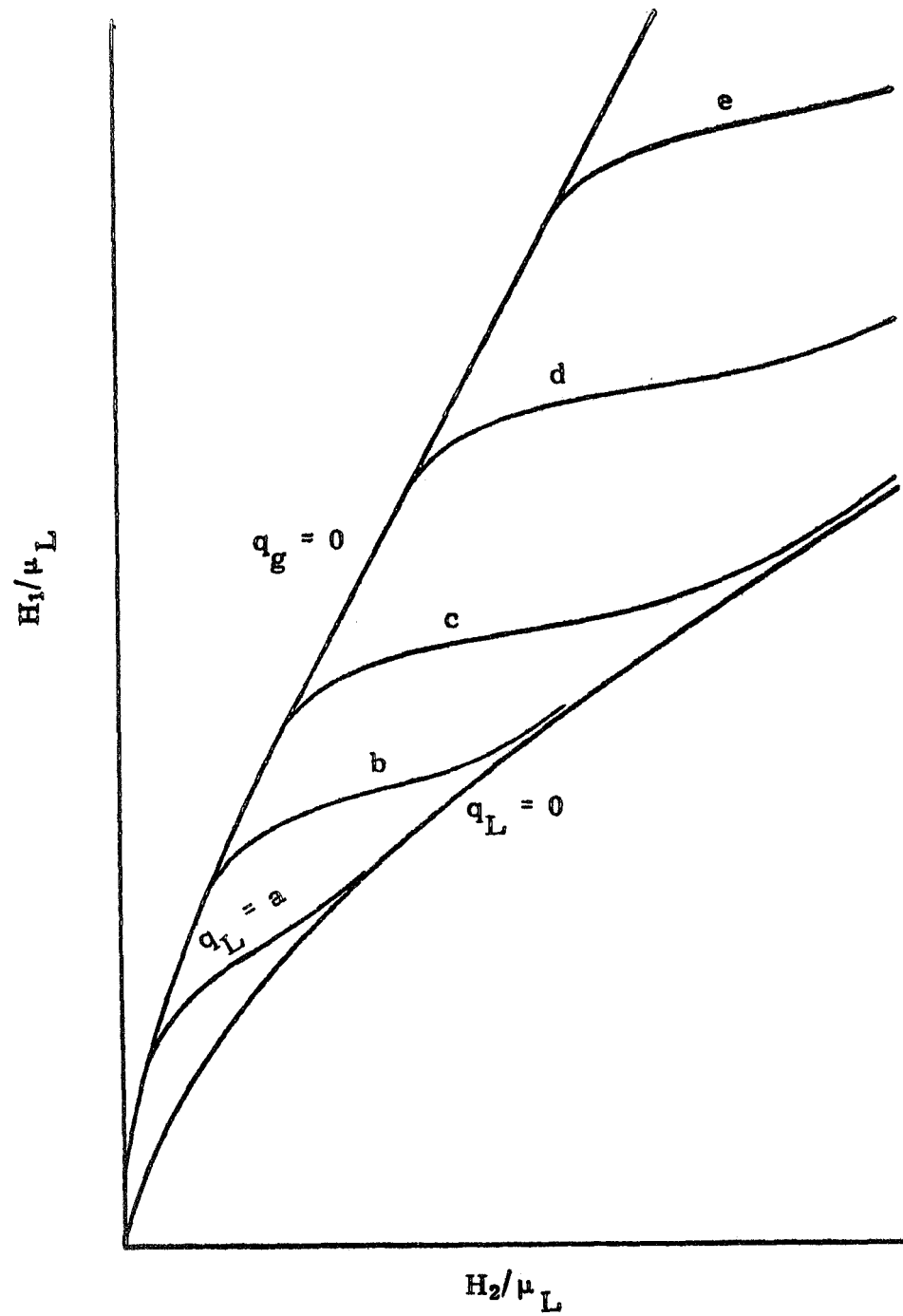


Figure 23. Idealized Calibration Data

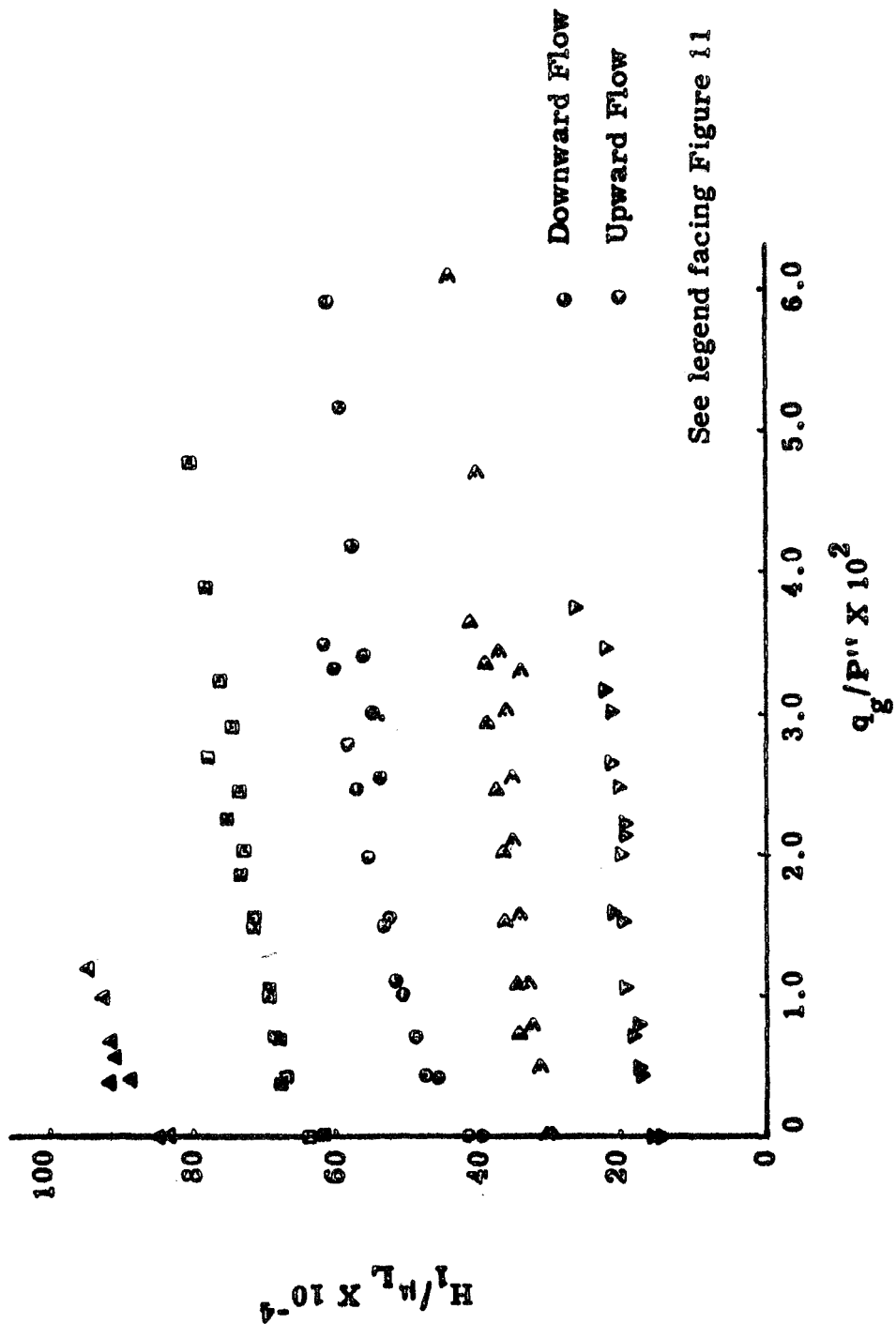


Figure 24. Experimental Data - Configuration IV, Cartridge No. 1

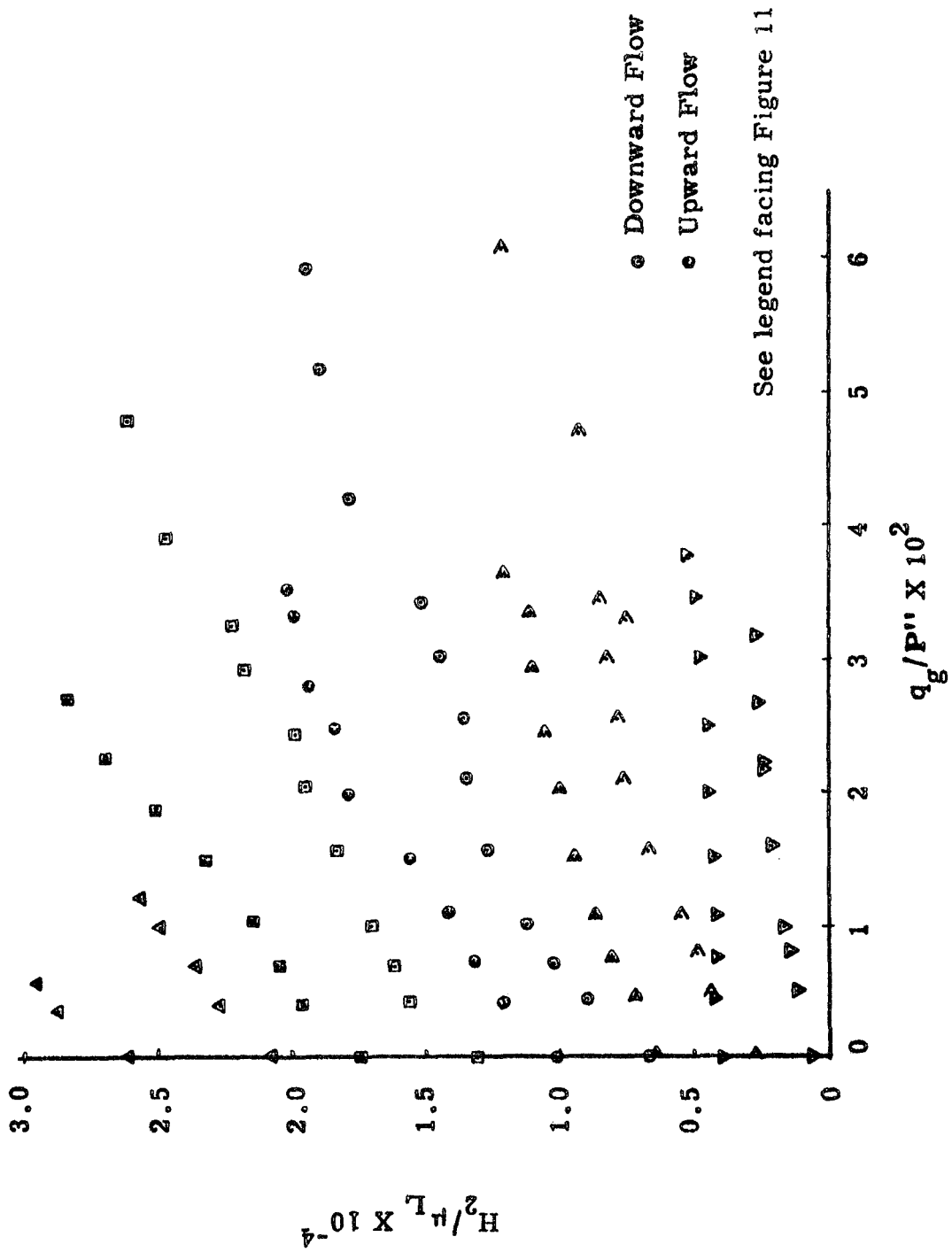


Figure 25. Experimental Data - Configuration IV, Cartridge No. 2

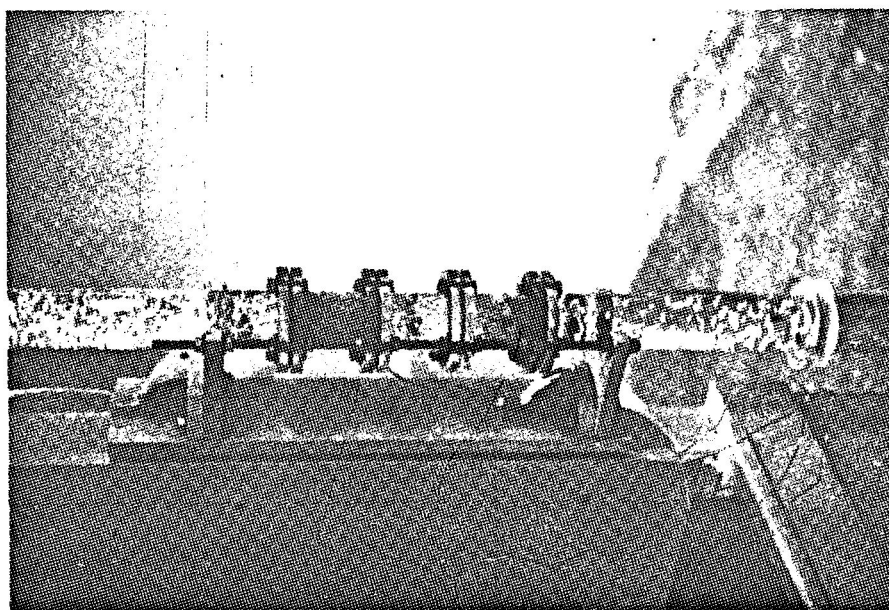
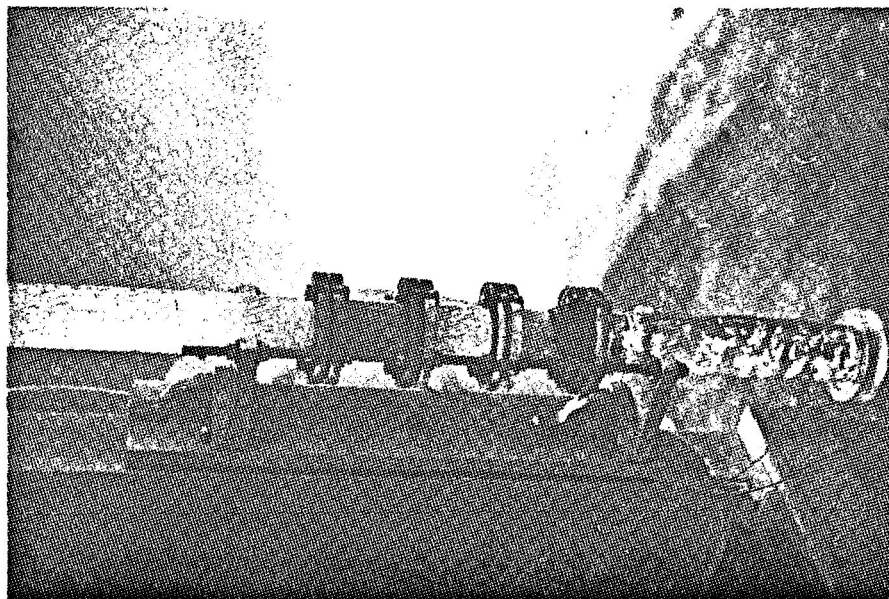
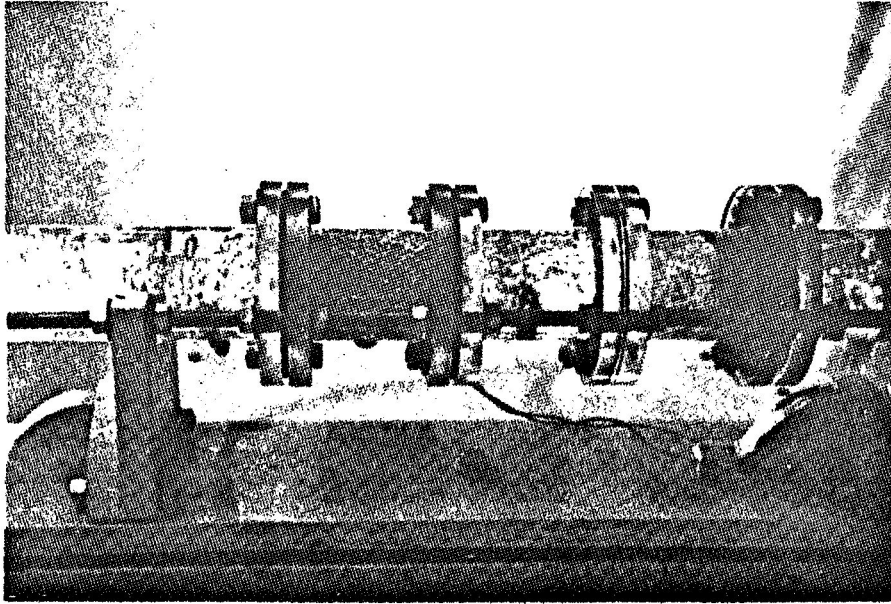
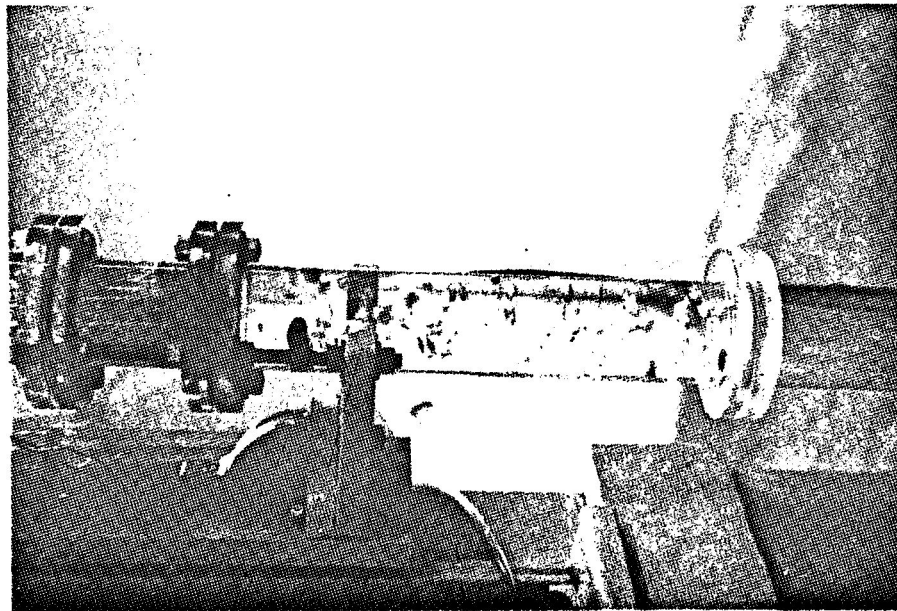


Figure 26. Photographs of the Test Section in Upward Two-Phase Flow



Porous Cartridges



Gas Injector

Figure 27. Photographs of Upward Two-Phase Flow

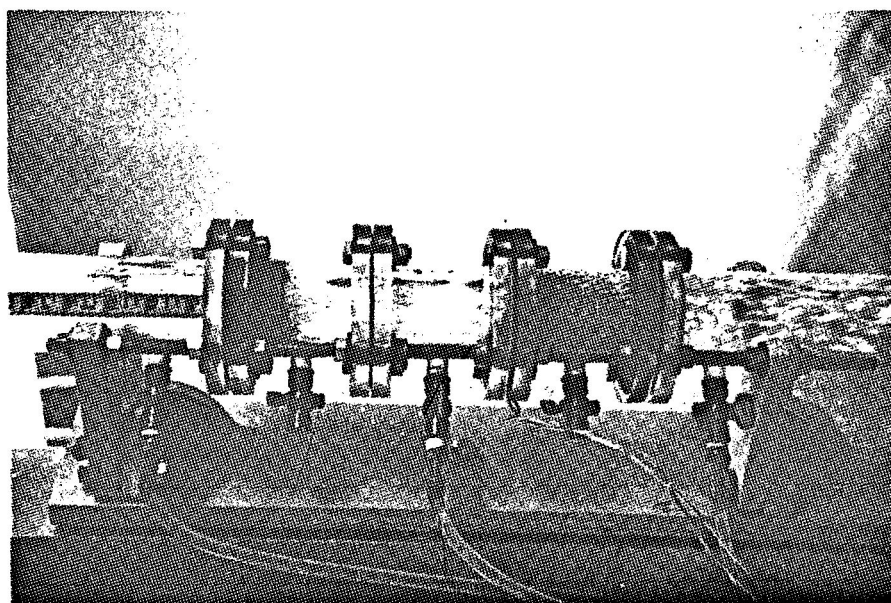
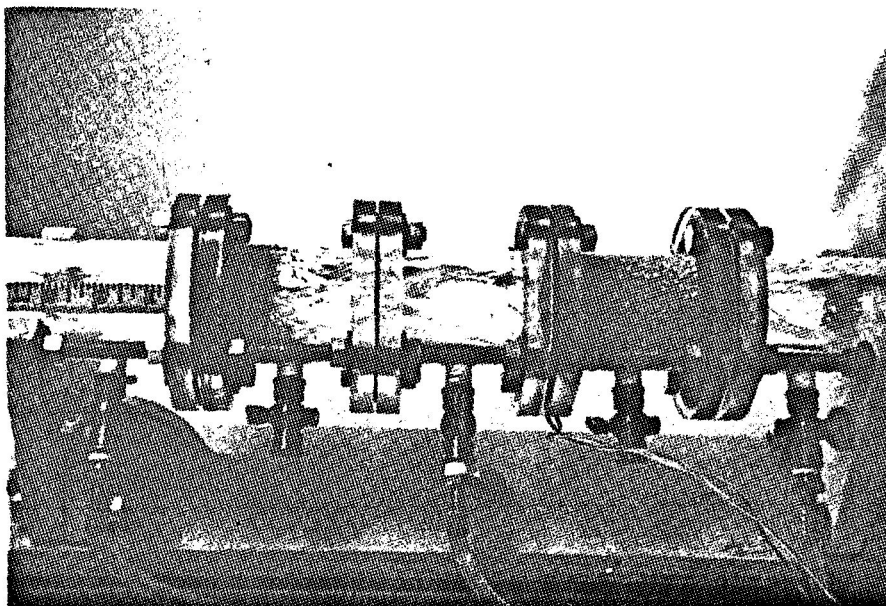


Figure 28. Photographs of the Porous Cartridges in Downward Two-Phase Flow

BIBLIOGRAPHY

1. Alspach, W. J., Miller, C. E., and Flynn, T. M. "Flow Measurement-Part 2, Mass Flowmeters in Cryogenics," Mechanical Engineering, Vol. 89 (May, 1967), pp. 105-113.
2. Collins, R. E. Flow of Fluids Through Porous Materials. New York: Reinhold Publishing Corporation, 1961.
3. Gorring, Robert L., and Katz, Donald L. "Bubble Rise in a Packed Bed Saturated with Liquids," American Institute of Chemical Engineering Journal, Vol. 8, No. 1, pp. 123-126.
4. Henry, Harold R. "Salt Intrusion into Fresh-water Aquifers," Journal of Geophysical Research, Vol. 64, No. 11, pp. 1911-1920, 1959.
5. Henry, Harold R. "Salt Intrusion into Coastal Aquifers," International Association for Scientific Hydrology, Publication No. 52, pp. 478-487, 1961.
6. Henry, Harold R. "Transitory Movements of the Salt-water Front in an Extensive Artesian Aquifer," U. S. Geological Survey Professional Paper 450-B, pp. 34-35, 1962.
7. Henry, Harold R. The Effects of Temperature and Density Gradients upon the Movement of Contaminants in Saturated Aquifers, Final Report, University of Alabama, 1966.
8. Henry, Harold R., Chow, Allan S., and Bates, P. E. Unpublished Notes, University of Alabama, 1967.

9. Lockhart, R. W. and Martinelli, R. C. "Proposed Correlation of Data for Isothermal Two-Phase, Two-Component Flow in Pipes," Chemical Engineering Progress, Vol. 45, No. 1, pp. 39-48.
10. Miller, David E. An Experimental Study of the Effects of Temperature and Density Gradients on Flow in Porous Material, M. S. Thesis, University of Alabama, 1966.
11. Moody, F. J. "Maximum Flow Rate of a Single Component, Two-Phase of Mixture," Transactions of ASME Journal of Heat Transfer (Feb. 1965), pp. 134-142.
12. Nicklin, D. J. "Two-phase Bubble Flow," Chemical Engineering Science, Vol. 17 (1962), pp. 693-702.
13. Scheidegger, Adrian E. The Physics of Flow Through Porous Media. New York: The Macmillian Company, 1960.
14. Soo, S. L. Fluid Dynamics of Multiphase Systems. Waltham, Massachusetts: Blasidell Publishing Company, 1967.
15. Tong, L. S. Boiling Heat Transfer and Two-Phase Flow. New York: John Wiley & Sons, Inc., 1965.
16. Weekman, Vern W., Jr. and Myers, John E. "Fluid-Flow Characteristics of Concurrent Gas-Liquid Flow in Packed Beds," American Institute of Chemical Engineering, Vol. 10, No. 6, pp. 951-957.
17. Wyllie, M. R. and Gardner, G. H. F. "The Generalized Kozeny-Carman Equation; Its Application to Problems of Multiphase Flow in Porous Media, Part 1 - Review of Existing Theories," World Oil (March, 1958), pp. 121-128.
18. Wyllie, M. R. and Gardner, G. H. F. "The Generalized Kozeny-Carman Equation; Its Application to Problems of Multiphase Flow in Porous Media, Part 2 - A Novel Approach to Problems of Fluid Flow," World Oil (April, 1958), pp. 210-227.

ADDITIONAL DATA

This section contains data and graphs for a configuration that was tested after the preceding part of this report was completed. Study of the preceding data led to the hypothesis that in order for a given meter to yield data which would plot in charts such as Figures 19 and 20 with a marked difference between curves for each liquid flow rate, it would be desirable for the flow to be laminar through one cartridge and turbulent through the other. Therefore the configuration illustrated in Figure 29 was constructed and tested.

The two-phase mixture was forced first through the one-half inch thick, cartridge of two inches diameter filled with 0.88 mm. glass beads. The small bead size and large cross sectional area contributed to a small Reynolds number based on mean velocity and bead diameter. The second cartridge was three inches thick and one-half inch diameter filled with 3 mm. glass beads. The larger bead size and the smaller cross section contributed to a larger Reynolds number.

The graph in Figure 30 is gas (air) flow rate plotted against pressure drop divided by liquid viscosity for the upper porous cartridge. An experimental curve has been drawn for each of four different liquid (water) flow rates. Figure 31 shows the same type of plot for the

lower porous cartridge. Figure 32 is a summary graph or chart in which the pressure drop divided by liquid viscosity for one cartridge has been plotted against the corresponding value of the same quantity for the other cartridge with liquid flow rate as the curve parameter. An additional family of curves with gas flow rate as the curve parameter has been superimposed on Figure 32 by taking the data off Figures 30 and 31. The two families of curves, for constant liquid flow rate and constant gas flow rate make this a complete calibration chart for the use of this meter with air and water. Of course, the calibration is useful only in the range of flow rates where curves of a given family do not overlap with other curves of the same family.

It should be noted that if in another situation the absolute pressure and temperature in the meter is different from that given herein the calibration will be different because the mechanics of flow in the porous beds is dependent on the volume rate of gas flow. In this case of this data the temperature was 75° F and the absolute pressure was 14.7 psi on the discharge end of the meter.

The overlap of the curves on the right of Figure 32 and the general single linear trend for the resulting composite group of data points indicate that the flow through one porous cartridge is dynamically similar to the flow through the other cartridge in this region. Under this condition of dynamic similarity the device cannot be used as a flow meter.

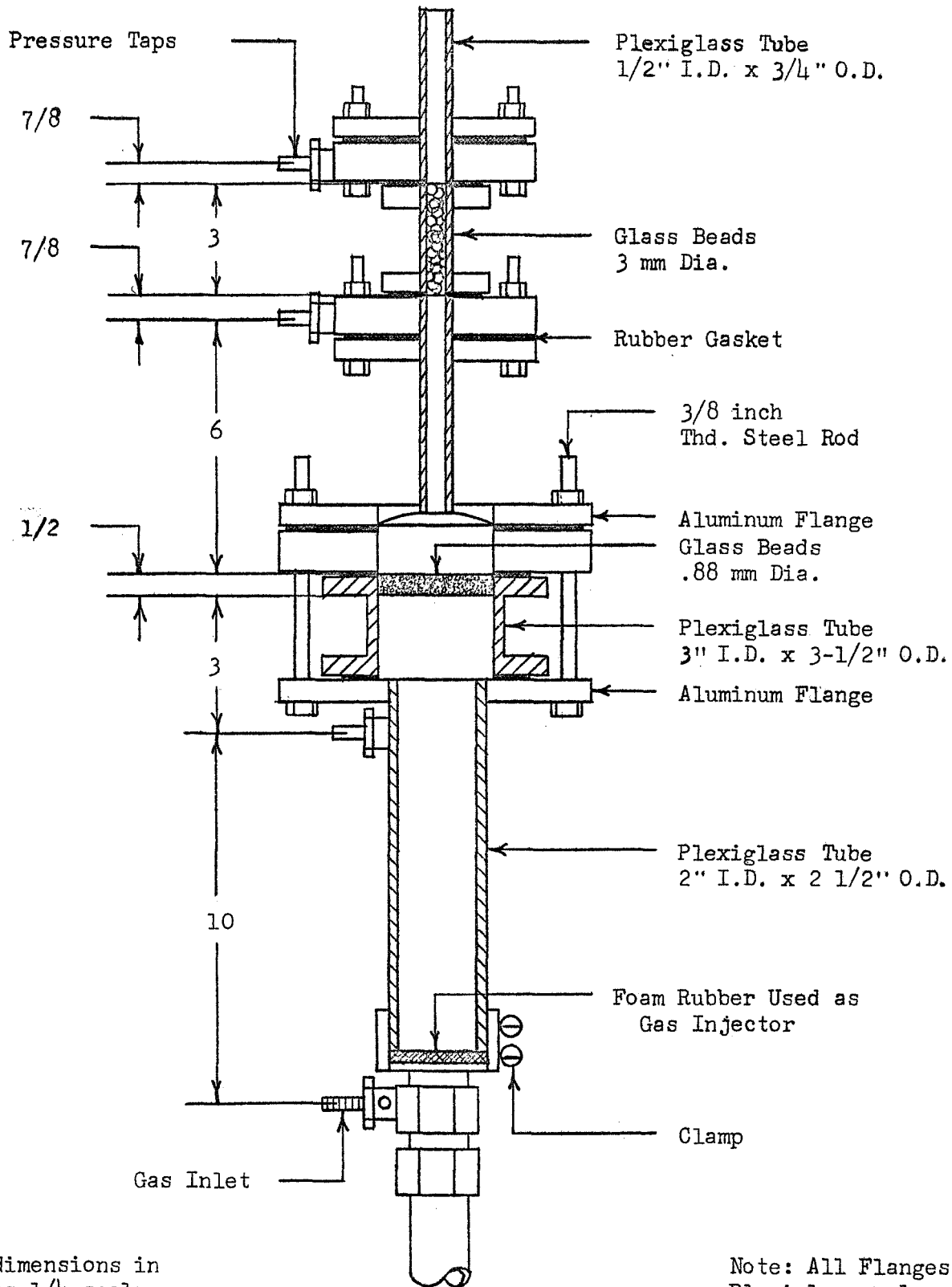
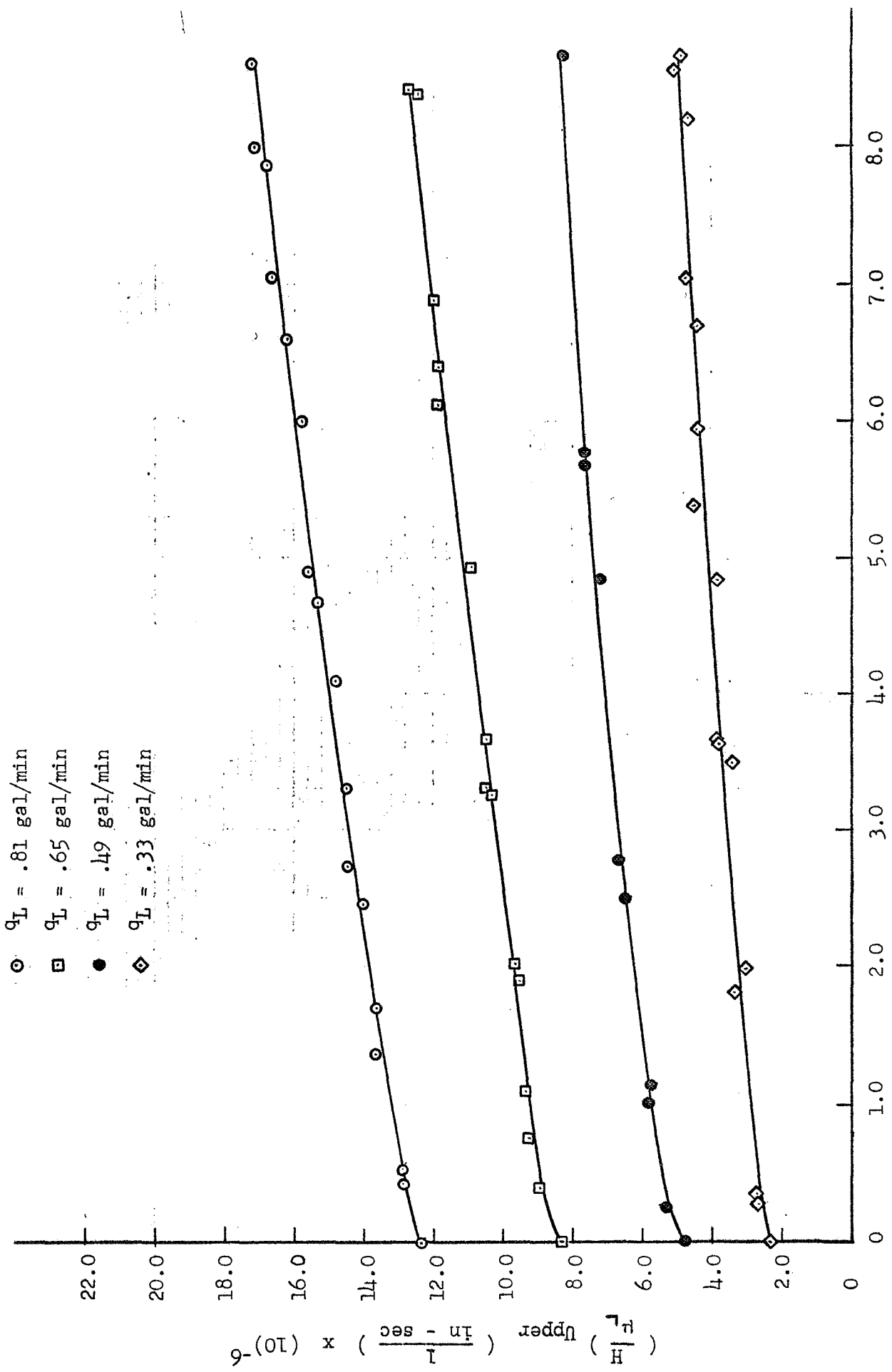
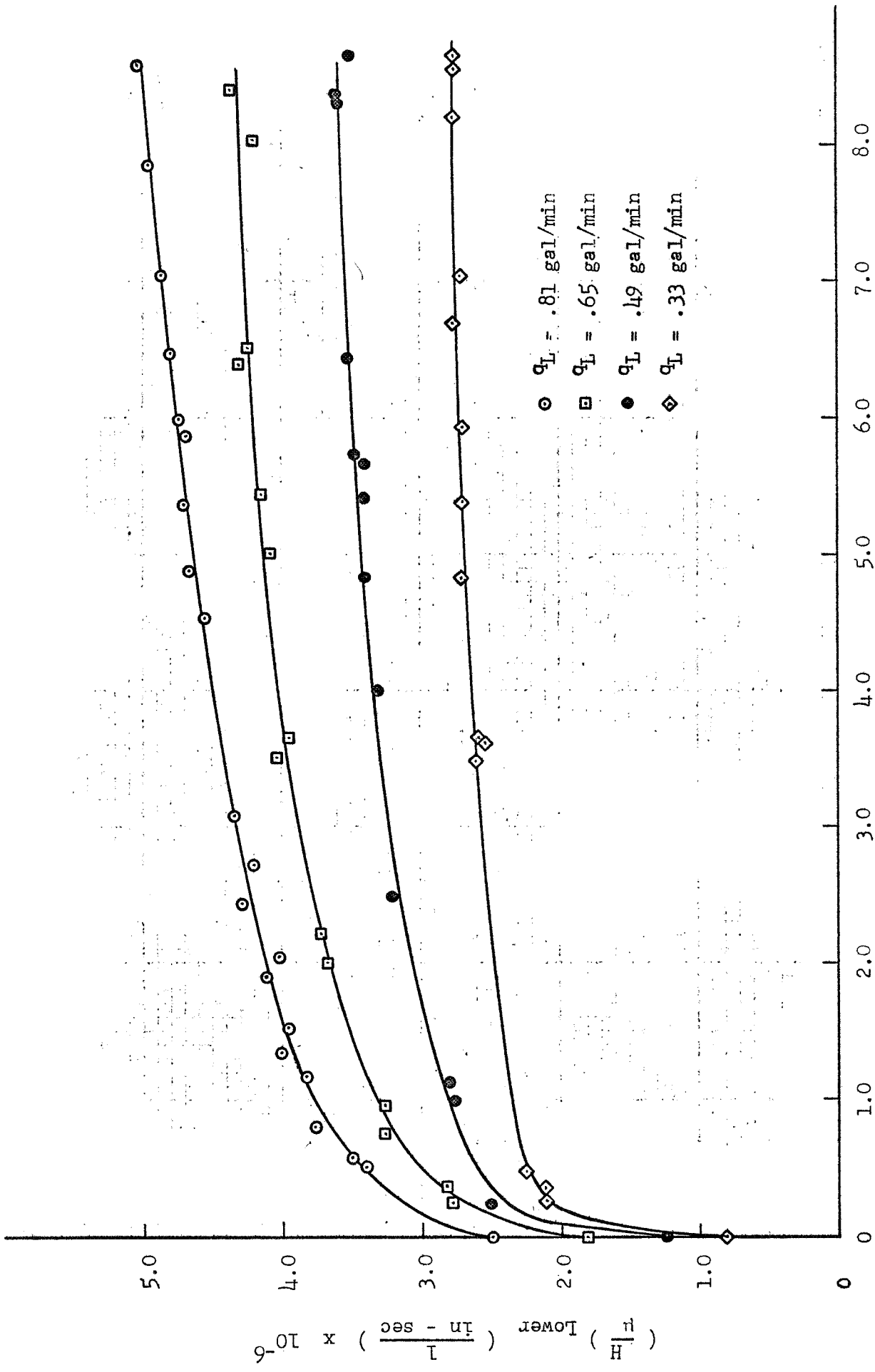


Figure 29. Meter with Porous Cartridges of Different Diameters.



Gas Flowrate, q_g (standard ft³/min) $\times 10^{-2}$
 Figure 30. Experimental Data for Meter of Figure 29.



Gas Flowrate, q_g (standard ft³/min) × 10⁻²
 Figure 31. Experimental Data for Meter of Figure 29.

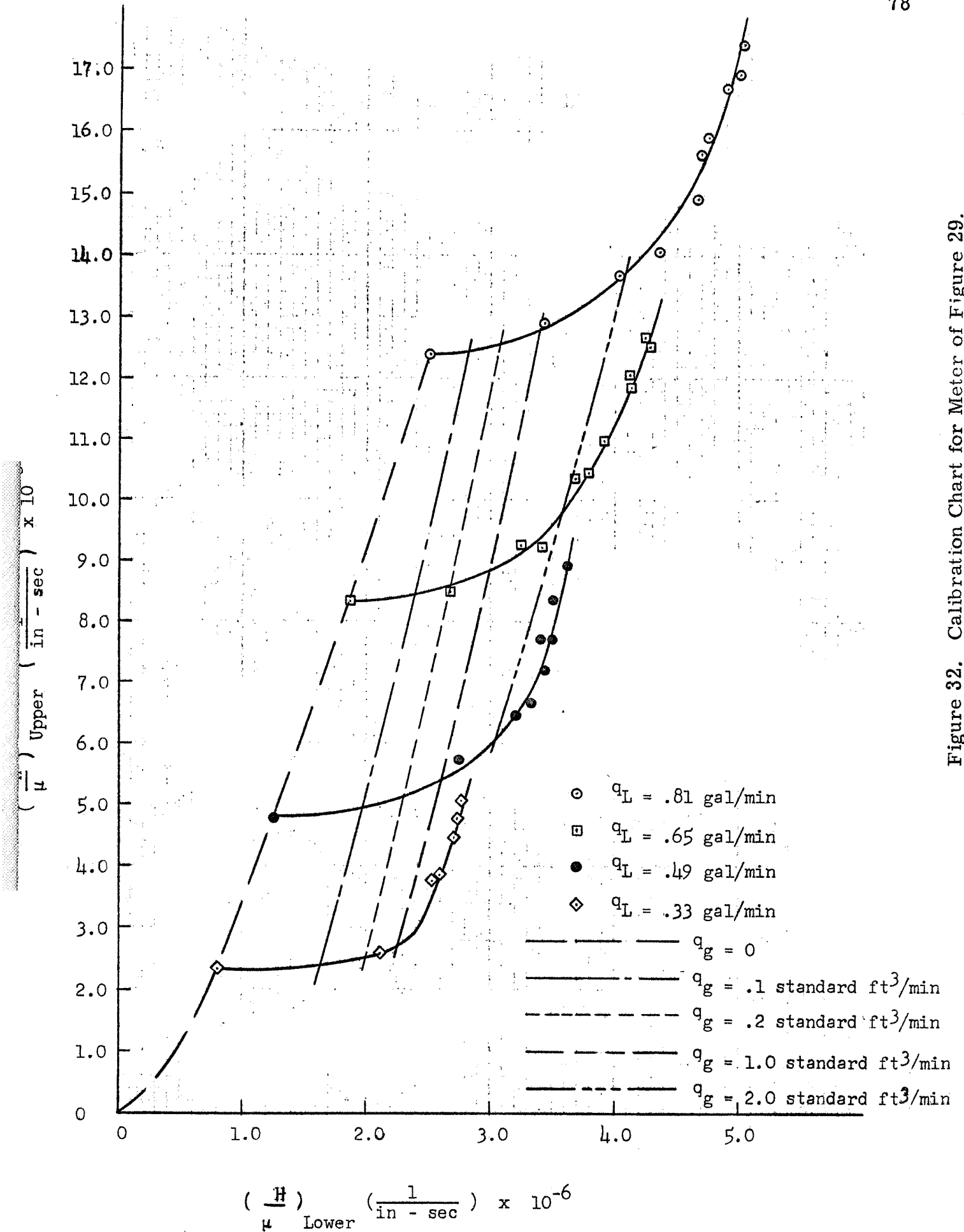


Figure 32. Calibration Chart for Meter of Figure 29.